AMERICAN SOCIETY FOR MICROBIOLOGY | Journal of Virology®

PATHOGENESIS AND IMMUNITY

Simian-Human Immunodeficiency Virus SHIV.CH505-Infected Infant and Adult Rhesus Macaques Exhibit Similar Env-Specific Antibody Kinetics, despite Distinct T-Follicular Helper and Germinal Center B Cell Landscapes

Ashley N. Nelson,[a] Ria Goswami,[a] Maria Dennis,[a] Joshua Tu,[a] Riley J. Mangan,[a] Pooja T. Saha,[b,c] Derek W. Cain,[a] Alan D. Curtis,[c,e] Xiaoying Shen,[a] George M. Shaw,[d] Katharine Bar,[d] Michael Hudgens,[b,c] Justin Pollara,[a] Kristina De Paris,[c,e] Koen K. A. Van Rompay,[f] Sallie R. Permar[a]

[a]Human Vaccine Institute, Duke University Medical Center, Durham, North Carolina, USA
[b]Gillings School of Public Health, University of North Carolina at Chapel Hill, Chapel Hill, North Carolina, USA
[c]Center for AIDS Research, School of Medicine, University of North Carolina at Chapel Hill, Chapel Hill, North Carolina, USA
[d]Department of Medicine, University of Pennsylvania, Philadelphia, Pennsylvania, USA
[e]Department of Microbiology and Immunology, School of Medicine, University of North Carolina at Chapel Hill, Chapel Hill, North Carolina, USA
[f]California National Primate Research Center, University of California, Davis, Davis, California, USA

ABSTRACT Global elimination of pediatric human immunodeficiency virus (HIV) infections will require the development of novel immune-based approaches, and understanding infant immunity to HIV is critical to guide the rational design of these intervention strategies. Despite their immunological immaturity, chronically HIV-infected children develop broadly neutralizing antibodies (bnAbs) more frequently and earlier than adults do. However, the ontogeny of humoral responses during acute HIV infection is poorly defined in infants and challenging to study in human cohorts due to the presence of maternal antibodies. To further our understanding of age-related differences in the development of HIV-specific immunity during acute infection, we evaluated the generation of virus-specific humoral immune responses in infant ($n = 6$) and adult ($n = 12$) rhesus macaques (RMs) infected with a transmitted/founder (T/F) simian-human immunodeficiency virus (SHIV) (SHIV.C.CH505 [CH505]). The plasma HIV envelope-specific IgG antibody kinetics were similar in SHIV-infected infant and adult RMs, with no significant differences in the magnitude or breadth of these responses. Interestingly, autologous tier 2 virus neutralization responses also developed with similar frequencies and kinetics in infant and adult RMs, despite infants exhibiting significantly higher follicular T helper cell (Tfh) and germinal center B cell frequencies than adults. Finally, we show that plasma viral load was the strongest predictor of the development of autologous virus neutralization in both age groups. Our results indicate that the humoral immune response to SHIV infection develops with similar kinetics among infant and adult RMs, suggesting that the early-life immune system is equipped to respond to HIV-1 and promote the production of neutralizing HIV antibodies.

IMPORTANCE There is a lack of understanding of how the maturation of the infant immune system influences immunity to HIV infection or how these responses differ from those of adults. Improving our knowledge of infant HIV immunity will help guide antiviral intervention strategies that take advantage of the unique infant immune environment to successfully elicit protective immune responses. We utilized a rhesus macaque model of SHIV infection as a tool to distinguish the differences in HIV humoral immunity in infants versus adults. Here, we demonstrate that the kinetics and quality of the infant humoral immune response to HIV are highly compara-

Citation Nelson AN, Goswami R, Dennis M, Tu J, Mangan RJ, Saha PT, Cain DW, Curtis AD, Shen X, Shaw GM, Bar K, Hudgens M, Pollara J, De Paris K, Van Rompay KKA, Permar SR. 2019. Simian-human immunodeficiency virus SHIV.CH505-infected infant and adult rhesus macaques exhibit similar Env-specific antibody kinetics, despite distinct T-follicular helper and germinal center B cell landscapes. J Virol 93:e00168-19. https://doi.org/10.1128/JVI.00168-19.

Editor Frank Kirchhoff, Ulm University Medical Center

Address correspondence to Sallie R. Permar, sallie.permar@duke.edu.

A.N.N. and R.G. contributed equally to this work.

Received 31 January 2019
Accepted 2 May 2019
Accepted manuscript posted online 15 May 2019
Published 17 July 2019

ble to those of adults during the early phase of infection, despite distinct differences in their Tfh responses, indicating that slightly different mechanisms may drive infant and adult humoral immunity.

KEYWORDS animal model, SHIV, SIV, human immunodeficiency virus, macaque, pediatric HIV, pediatric immunology

Despite the widespread availability of antiretroviral (ARV) therapy (ART) for human immunodeficiency virus (HIV)-infected pregnant women, approximately 180,000 infants were newly infected in 2017 due to issues of treatment access and adherence and acute maternal HIV infection (1). While the developing immune system and lack of immunological memory during early infancy can render neonates more susceptible to infections, they may also provide an opportunity for unique interventions. Furthermore, HIV immunization in infancy could be an opportunity to both interrupt postnatal transmission to breastfeeding infants, the current most common mode of infant HIV infection (2), as well as elicit lifelong HIV immunity prior to the renewed HIV acquisition risk upon sexual debut. A better understanding of how the infant's developing immune system influences disease outcome and pathogenesis during HIV infection and how it compares to that of adults is imperative to inform the design and evaluation of pediatric intervention therapies and vaccination strategies.

The disease course in HIV-infected infants is dramatically different from that in HIV-infected adults and can be further differentiated depending on the route of transmission (3, 4). Without treatment, vertically HIV-infected infants tend to have high plasma viral RNA (vRNA) loads, experience rapid declines in peripheral $CD4^+$ T cell counts, and progress to AIDS rapidly compared to adults (5, 6). Transmission studies have indicated that infants infected during breastfeeding tend to have a better clinical outcome than perinatally infected infants do. Specifically, postnatal HIV-infected infants have a low risk of mortality within the first 18 months of infection (7), increased median survival times from infection (8), and high long-term survival rates (9, 10) compared to infants who acquire HIV infection perinatally. The ontogeny of HIV Env-specific antibodies (Abs) is also quite different between infants and adults, and understanding these differences could inform infant HIV Env vaccine development and evaluation. In HIV-infected adults, Env-specific antibodies are detectable by approximately 14 days after infection (11). Yet the early kinetics of HIV-exposed and -infected infants' natural IgG responses are masked by placentally acquired maternal antibody. More importantly, increases in HIV-specific IgG responses from 6 months through the first year of life have been implicated in a better clinical outcome (12, 13). Recent studies have indicated that chronically HIV-infected infants frequently develop broadly neutralizing antibodies (bnAbs) during early life (range, 11.4 to 28.2 months) and that they do so much more rapidly than adults (14). Interestingly, Env-specific IgG levels were significantly associated with neutralizing antibody breadth in HIV-infected infants (15). Furthermore, a bnAb isolated from an infected infant exhibited lower levels of somatic hypermutation (SHM) than adult-isolated bnAbs, with similar potency and breadth (14, 16, 17). Despite the early development of bnAbs in infants, the presence of antibodies capable of mediating antibody-dependent cellular cytotoxicity (ADCC) has been reported to be delayed in infants infected during the first 6 weeks of life yet is associated with a better outcome of disease (18, 19). These differences in infant and adult HIV infection further support a need to better characterize pediatric HIV humoral immunity. While studies in human cohorts have improved our understanding of the differences in the infant and adult immune responses during chronic HIV infection, the presence of maternal antibodies limits our ability to study the plasma HIV-specific antibody responses during the acute phase of infection in infants.

Experimental infection of nonhuman primates (NHPs) with chimeric simian-human immunodeficiency virus (SHIV) remains an invaluable model for studying HIV pathogenesis and evaluating therapeutic and prevention strategies. In addition, the rhesus macaque (RM)-SHIV model can be used to define differences in the ontogeny of

TABLE 1 Infant and adult SHIV.C.CH505-infected monkey cohort information, weeks of challenges to infection, and age at infection

Group and animal ID[a]	Sex[b]	Weeks of challenges to infection	Age at infection
Infants (oral challenge)			
46346	F	2	9 wk
46352	F	2	9 wk
46357	M	1	5 wk
46359	F	3	10 wk
46367	M	7	14 wk
46380	F	4	11 wk
Adults (i.v. challenge)			
39472	F	1	8 yr
42870	F	1	5 yr
41919	F	1	6 yr
43068	F	1	5 yr
43268	F	1	4 yr
42814	F	1	5 yr
42368	F	1	5 yr
43633	F	1	4 yr
39950	F	1	8 yr
41522	F	1	6 yr
38200	F	1	10 yr
41672	F	1	6 yr

[a]i.v., intravenous.
[b]F, female; M, male.

immune responses directed against HIV between infants and adults. We have utilized this model to study adult and infant humoral immune responses to acute infection with SHIV.C.CH505, a clinically relevant SHIV expressing the Env glycoprotein of the HIV-1 transmitted/founder (T/F) CH505 (subtype C) virus, isolated from an HIV-infected adult who developed plasma bnAb activity (20–22). A mutation within the CD4 binding site of this SHIV Env facilitates enhanced interaction with the rhesus CD4 molecule (20). More importantly, SHIV.C.CH505 can infect and replicate efficiently in rhesus macaques and exhibit plasma viral load kinetics in macaques similar to those seen in acute HIV-1 infections in humans (20). Using this highly relevant infection model, we conducted a longitudinal analysis of the virus-specific humoral immune response in SHIV.C.CH505-infected infant and adult monkeys and defined the virologic and immunologic features that are associated with the development of plasma neutralization activity in each age group. This work will allow us to improve our understanding of age-related differences in HIV Env-specific B cell immunity elicited during acute infection, which can guide the development of infant vaccine strategies that can optimally prime B cells for virus-neutralizing responses.

(This article was submitted to an online preprint archive [23].)

RESULTS

Infant and adult RMs exhibit similar plasma viral load kinetics following SHIV.C.CH505 infection. Twelve female, adult rhesus macaques (age range, 4 to 10 years) (Table 1) were infected intravenously with SHIV.C.CH505 at a dose of 3.4×10^5 50% tissue culture infective doses ($TCID_{50}$). All 12 adult monkeys became infected after the first inoculation. To mimic breast milk transmission, six infant rhesus macaques were infected orally starting at 4 weeks of age (Table 1) with a repeated-exposure regimen that has been successfully developed with simian immunodeficiency virus SIV_{mac251} to simulate exposure to HIV by breastfeeding (24, 25). Once monkeys were infected, viremia peaked at 2 weeks in both age groups, and peak viremias were of similar magnitudes between the groups (infant range, 6.7×10^5 to 3.2×10^7 vRNA copies/ml of plasma; adult range, 3×10^5 to 1.3×10^7 vRNA copies/ml of plasma) (Fig. 1A). The range in peak viremia among both age groups was similar to those observed in acute SIV (25, 26) and HIV (27) infections. At 12 weeks postinfection (wpi), 11 of the 12 adult monkeys

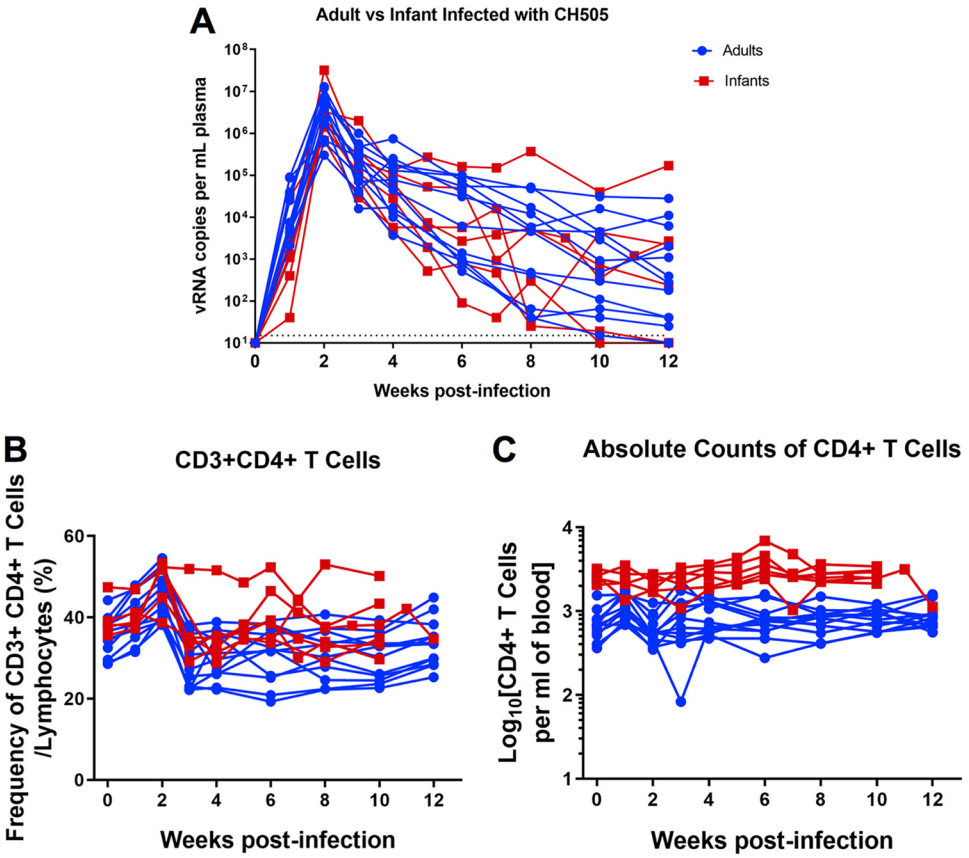

FIG 1 Plasma viral loads and CD4$^+$ T cell frequencies in adult and infant monkeys following SHIV.C.CH505 infection. (A) Plasma viral loads were monitored weekly or biweekly through 12 wpi. (B and C) Automated complete blood counts were collected weekly, and the proportion (B) and absolute counts per milliliter of blood (C) of CD4$^+$ T cells were determined. Each line represents one animal.

and 4 of the 6 infant monkeys maintained plasma viral loads above the limit of detection of the assay (15 vRNA copies/ml of plasma) (Fig. 1A). Both infant and adult monkeys exhibited a transient decrease in frequencies of CD4$^+$ T cells at 3 wpi (Fig. 1B); however, these frequencies were maintained through 12 wpi. Infant monkeys had higher absolute CD4 T cell counts overall than did adult monkeys, with ranges similar to those reported for uninfected cohorts (24, 28). Changes in CD4$^+$ T cell absolute counts were not observed over the course of SHIV infection in either age group (Fig. 1C); thus, the SHIV.C.CH505 virus exhibited a more attenuated phenotype in infant monkeys, in contrast to observations in the SIV_{mac251} model (29–31). Since the same viremic pattern was observed in both age groups independent of the route of infection, this model provided an opportunity to define differences in the infant and adult immune responses to SHIV infection.

The kinetics, magnitude, and specificity of HIV Env-specific plasma IgG responses are similar in infant and adult RMs during acute SHIV.C.CH505 infection. We measured HIV Env-specific antibody responses to evaluate whether the ontogeny of these responses would differ between the infant and adult monkeys during the acute phase of infection. In both groups, CH505 gp120-specific responses were detectable by 3 wpi, with no statistically significant difference in magnitude (median gp120 IgG levels in infants and adults of 1,297 ng/ml and 1,785 ng/ml, respectively [$P = 0.301$]) (Fig. 2A). These responses continued to increase through 12 wpi, with no significant difference in magnitude (median gp120 IgG levels in infants and adults of 1.3×10^5 ng/ml and 2.3×10^5 ng/ml, respectively [$P = 0.494$]) or kinetics between infants and adults (Fig. 2A). Overall, the kinetics and magnitude of the gp41-specific plasma IgG response were also not significantly different between both age groups

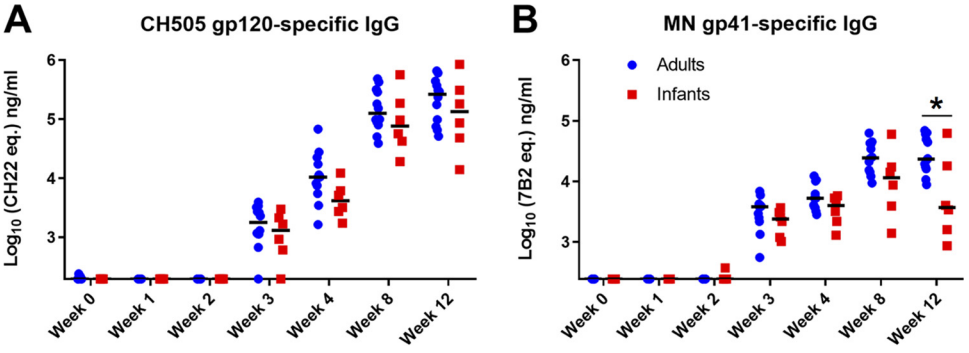

FIG 2 The kinetics and magnitude of HIV Env-specific IgG responses are similar in infant and adult monkeys during acute SHIV.C.CH505 infection. HIV CH505 gp120-specific (A) and MN gp41-specific (B) IgG responses in the plasma of adult and infant monkeys through 12 wpi are shown. Statistical analysis was performed using Wilcoxon rank sum tests with exact *P* values to compare IgG responses between SHIV-infected infant and adult monkeys, followed by adjustments for multiple comparisons. *, unadjusted *P* value of <0.05. All *P* values are >0.05 once adjusted for multiple comparisons (see Table S3 in the supplemental material for both unadjusted *P* and FDR *P* values for all comparisons). Medians are indicated as black horizontal lines on the dot plots.

(Fig. 2B). However, at 12 wpi, the infant monkeys exhibited a trend toward lower gp41-specific IgG responses than those of adults, although this difference was not significant after correction for multiple comparisons (median gp41 IgG levels in infants and adults at 12 wpi of 3,712 ng/ml and 23,305 ng/ml, respectively [$P = 0.041$; false discovery rate-adjusted *P* [FDR *P*] $= 0.458$]) (Fig. 2B).

To determine the specificity of the plasma Env-specific IgG responses between age groups, we used a binding antibody multiplex assay (BAMA) to assess binding to various HIV Env linear and conformational epitopes at week 4 (Fig. 3A) and week 12 (Fig. 3B) postinfection (Table 2). For both groups, anti-V3 and -C5 binding responses were dominant and increased from week 4 to week 12 (Fig. 3A and B). Although infant monkeys exhibited a slightly higher antibody specificity for the CD4 binding site at 12 wpi, these differences were not statistically significant ($P = 0.335$) (Fig. 3C). While anti-V2 responses were rarely detected by BAMAs (Fig. 3A and B), linear peptide microarray analysis demonstrated that these responses were primarily CH505 specific (Fig. 3D). We also used a BAMA to assess cross-clade gp120 and gp140 breadth at 4 and 12 wpi (Fig. 4A and B). At 12 wpi, antibodies from infants and adults recognized all nine gp120 and gp140 antigens tested, demonstrating breadth acquisition (Fig. 4B). Overall, the median gp120- and gp140-specific IgG responses across all clades trended higher at week 12 in adult monkeys, consistent with a higher gp41 plasma IgG binding response (Fig. 4B).

Functional T cell responses in infant and adult monkeys during the acute phase of SHIV.C.CH505 infection. We assessed functional T cell responses by measuring the frequency of interferon gamma (IFN-γ)-, interleukin-2 (IL-2)-, IL-17-, or tumor necrosis factor alpha (TNF-α)-producing $CD4^+$ and $CD8^+$ T cells. Due to limited sample availability, only peripheral blood mononuclear cells (PBMCs) collected from infant and adult monkeys at 8 wpi were analyzed (Fig. 5). Overall, the majority of $CD4^+$ and $CD8^+$ T cells from infants had little to no cytokine production compared to those from adults (Fig. 5A and B), similar to what has been observed in SIV and HIV infections (26, 32). When assessing the mean proportions of cytokine-producing T cells between both age groups, adult $CD4^+$ T cells predominantly produced IL-2, IL-17, or TNF-α, while infant $CD4^+$ T cells produced either IFN-γ, IL-2, or IL-17 (Fig. 5C). In contrast, $CD8^+$ T cells from both groups predominantly produced either IL-17 or TNF-α (Fig. 5D).

SHIV.C.CH505-infected infant monkeys have high proportions of T-follicular helper cells in the lymph node compared to those of adults. Frequencies of T-follicular helper (Tfh) cells have been reported to be increased in HIV-infected children compared to adults (33). In order to investigate Tfh cell responses during the acute phase of SHIV infection, we evaluated the proportions of CH505-specific and total

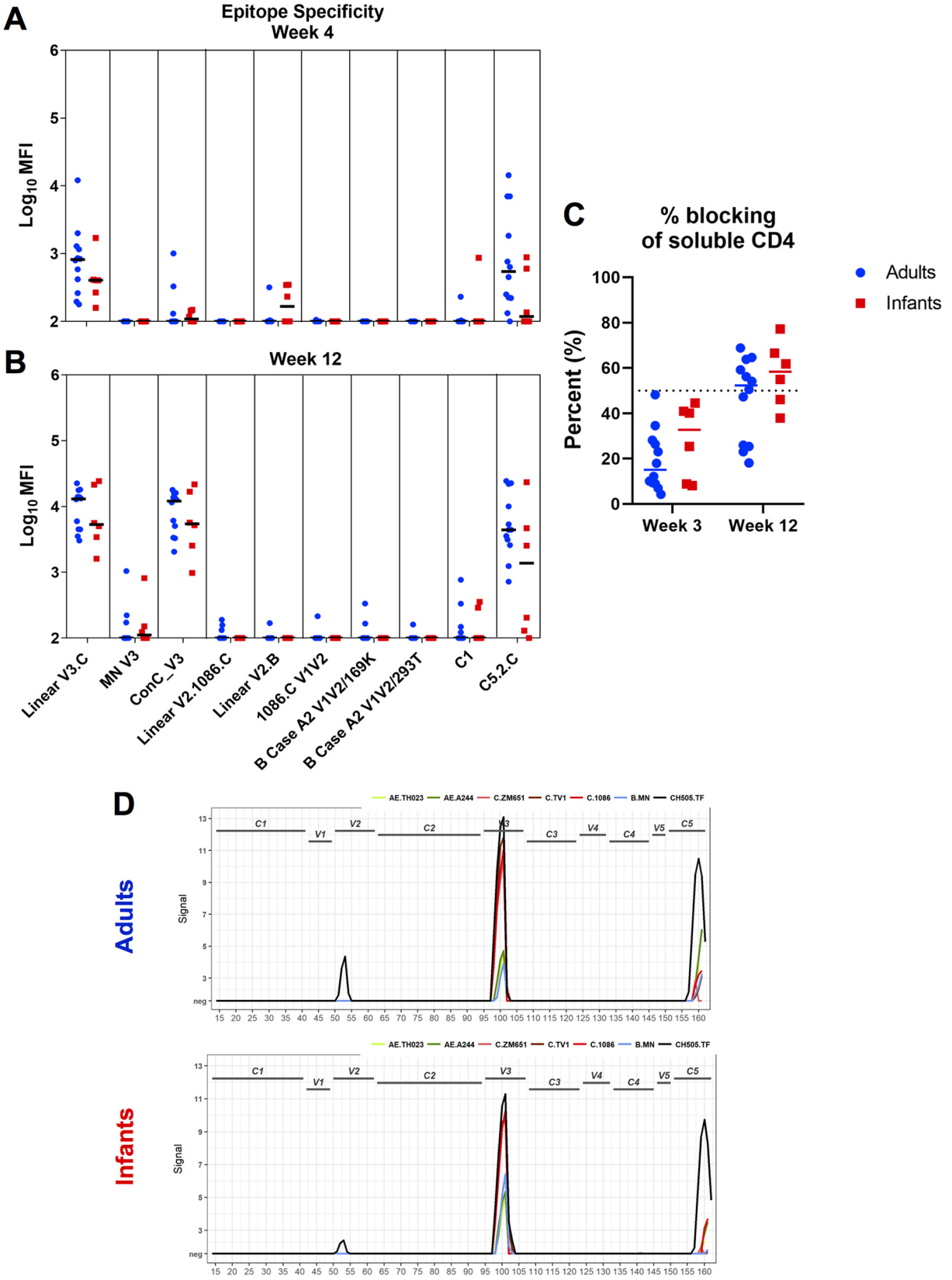

FIG 3 Similar specificities of Env-specific IgG responses during acute SHIV.C.CH505 infection in infants and adults. (A and B) Plasma IgG specificity against a panel of HIV Env linear and conformational epitopes at week 4 (A) and week 12 (B) postinfection. (C) Plasma blocking of soluble CD4-gp120 interactions at weeks 3 and 12 postinfection. Medians are indicated as horizontal lines on the dot plots. (D) Binding intensity to gp120-specific peptides of HIV strain-specific sequences. Peaks depict the group median signal intensity. neg, response did not meet the positivity call criteria.

TABLE 2 Linear epitopes targeted by binding antibodies in the study

Epitope	Peptide region[a]	Amino acid positions[b]
V2	52–53	160–177
V3	100–101	304–321
C5	159–161	493–513

[a]Peptide regions as defined in the micrography library.
[b]HXB2 numbering.

$CD4^+$ $CXCR5^{hi}$ $PD1^{hi}$ (Fig. 6A to D) Tfh cells in the lymph node of infant and adult monkeys at 12 wpi. The frequencies of total $CD4^+$ T cells were similar between the two age groups, and the proportion of CH505-specific Tfh cells was not significantly different between the two groups ($P = 0.592$), yet infants had significantly higher proportions of total $CD4^+$ $CXCR5^{hi}$ $PD1^{hi}$ Tfh cells ($P = 0.024$; FDR $P = 0.036$) (Fig. 6A to D). Additionally, we compared the frequencies of the Tfh subsets based on the surface expression of CXCR3 and CCR6, as follows: Tfh1 ($CXCR3^+$ $CCR6^-$), Tfh2 ($CXCR3^-$ $CCR6^-$), and Tfh17 ($CXCR3^-$ $CCR6^+$) (Fig. 6E and F). In all, adult monkeys exhibited a

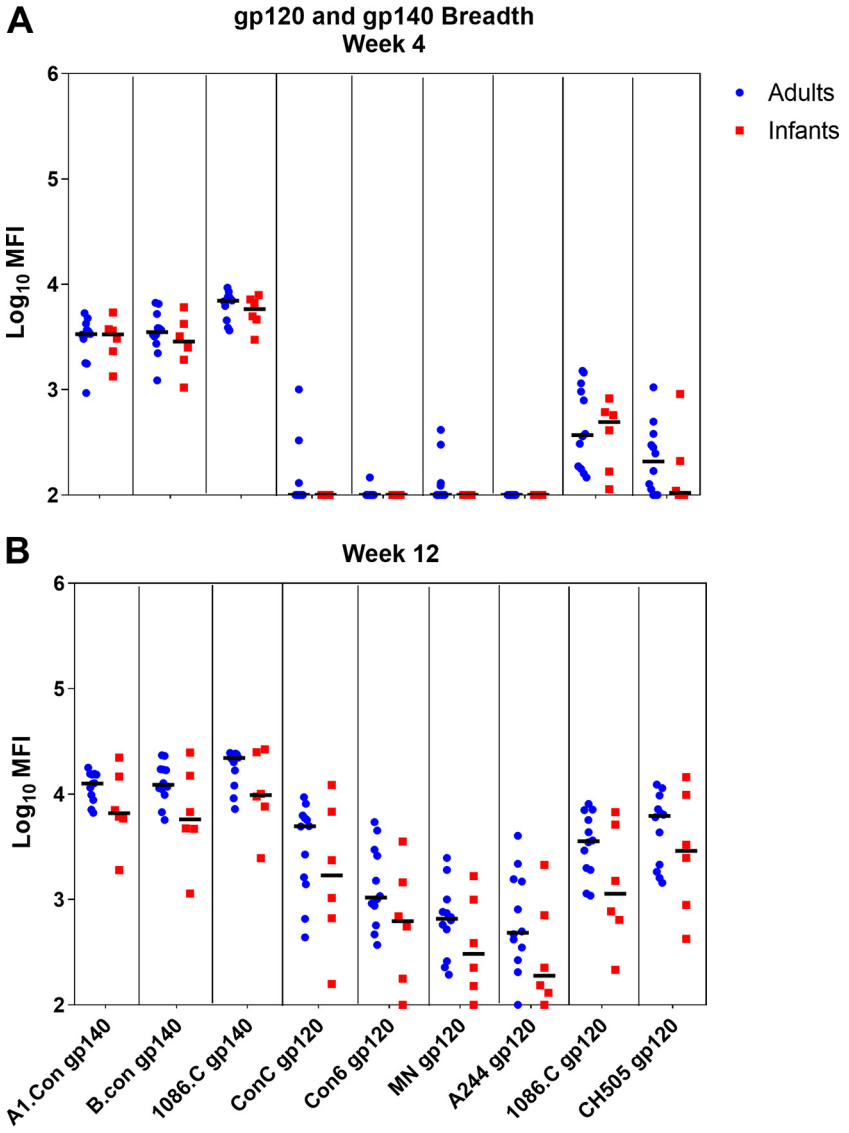

FIG 4 Adult and infant monkeys develop similar breadths of gp120 and gp140 IgG responses during acute SHIV.C.CH505 infection. Cross-clade HIV gp120 and gp140 IgG breadths at week 4 (A) and week 12 (B) postinfection are shown. Medians are indicated as horizontal lines on the dot plots.

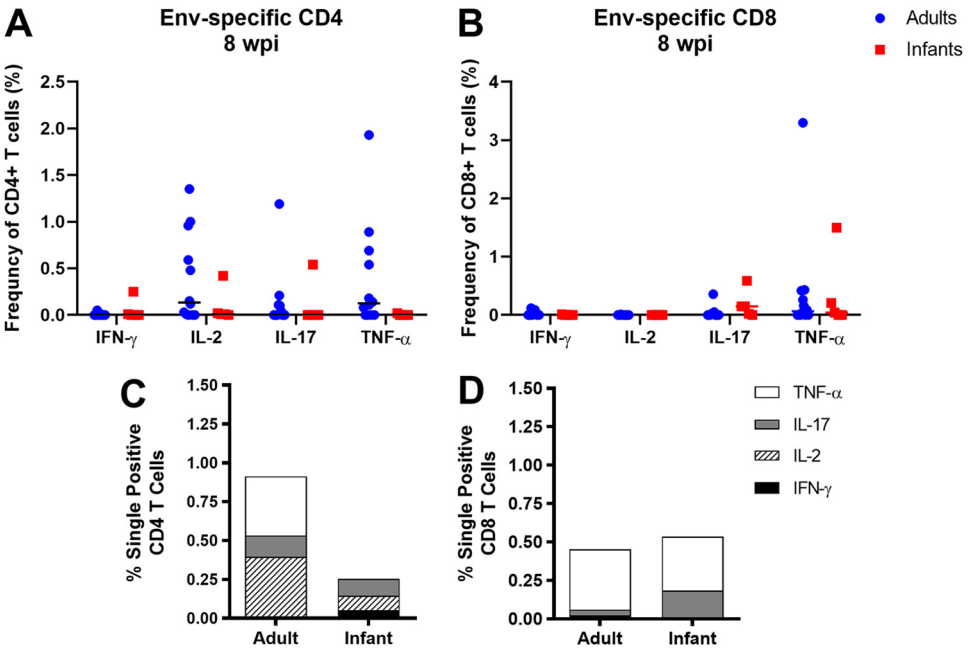

FIG 5 Env-specific $CD4^+$ and $CD8^+$ T cell responses in SHIV.C.CH505-infected infant and adult RMs. (A and B) Frequencies of HIV Env-specific $CD4^+$ (A) and $CD8^+$ (B) T cells expressing IFN-γ, IL-2, IL-17, or TNF-α in the periphery at 8 wpi. Each data point represents one animal, and medians are indicated as horizontal lines. (C and D) Bar graphs representing the mean proportions of $CD4^+$ (C) and $CD8^+$ (D) T cells expressing IFN-γ, IL-2, IL-17, or TNF-α in infant and adult monkeys.

significantly higher proportion of Tfh1 cells in the lymph node ($P = 0.013$; FDR $P = 0.021$) (Fig. 6E), while infants had a significantly higher proportion of Tfh17 cells ($P = 0.001$; FDR $P = 0.003$) (Fig. 6G) at 12 wpi. No significant difference was observed in Tfh2 proportions between the two age groups ($P = 0.066$) (Fig. 6F). Thus, SHIV-infected infant macaques exhibited a distinct Tfh landscape compared to adult macaques.

Proportions of CH505-specific memory B cells are similar between infant and adult monkeys. We evaluated systemic memory B cells in infant and adult monkeys at 0, 6, and 12 wpi (Fig. 7A and B). Additionally, we compared the frequencies of total B cells and germinal center (GC) B cells in lymph nodes at 12 wpi between both age groups (Fig. 7C to E). Due to a lack of sample availability, memory B cell populations at week 0 in the systemic compartment were evaluated in only 3 monkeys from each age group. Changes from the baseline in total memory B cells ($CD14^-$ $CD16^-$ $CD20^+$ IgD^- $CD27^+$) and CH505 gp120-specific memory B cells were not significantly different between age groups at 6 and 12 wpi ($P = 1$; 6 and 12 wpi for both parameters) (Fig. 7A and B). Similarly, the frequencies of total B cells ($CD3^-$ $CD20^+$) in lymph nodes were not significantly different ($P = 0.143$) (Fig. 7D) at 12 wpi. However, infants exhibited a significantly higher frequency of GC B cells, defined as $CD20^+$ $Bcl6^+$ $Ki67^+$ (Fig. 7C), than did adults ($P = 0.03$; FDR $P = 0.05$) (Fig. 7E), consistent with high proportions of Tfh cells in lymph nodes at 12 wpi (Fig. 6D).

SHIV.C.CH505-infected infant and adult monkeys develop comparable virus tier 2 autologous plasma neutralization responses. Since the kinetics, magnitude, and breadth of plasma HIV Env-specific IgG responses were similar between infant and adult monkeys, we next evaluated the HIV neutralization activity of these plasma IgG responses. We found that both age groups developed similar neutralization activity at 12 wpi against the tier 1 clade-matched isolates MW965 (50% infective dose [ID_{50}] ranges of 135 to 31,736 for infants and 324 to 4,949 for adults [$P = 0.384$]) (Fig. 8A) and CH505 w4.3 (ID_{50} ranges of 45 to 950 for infants and 45 to 750 for adults [$P = 0.605$]) (Fig. 8B). Furthermore, neutralization activity against the autol-

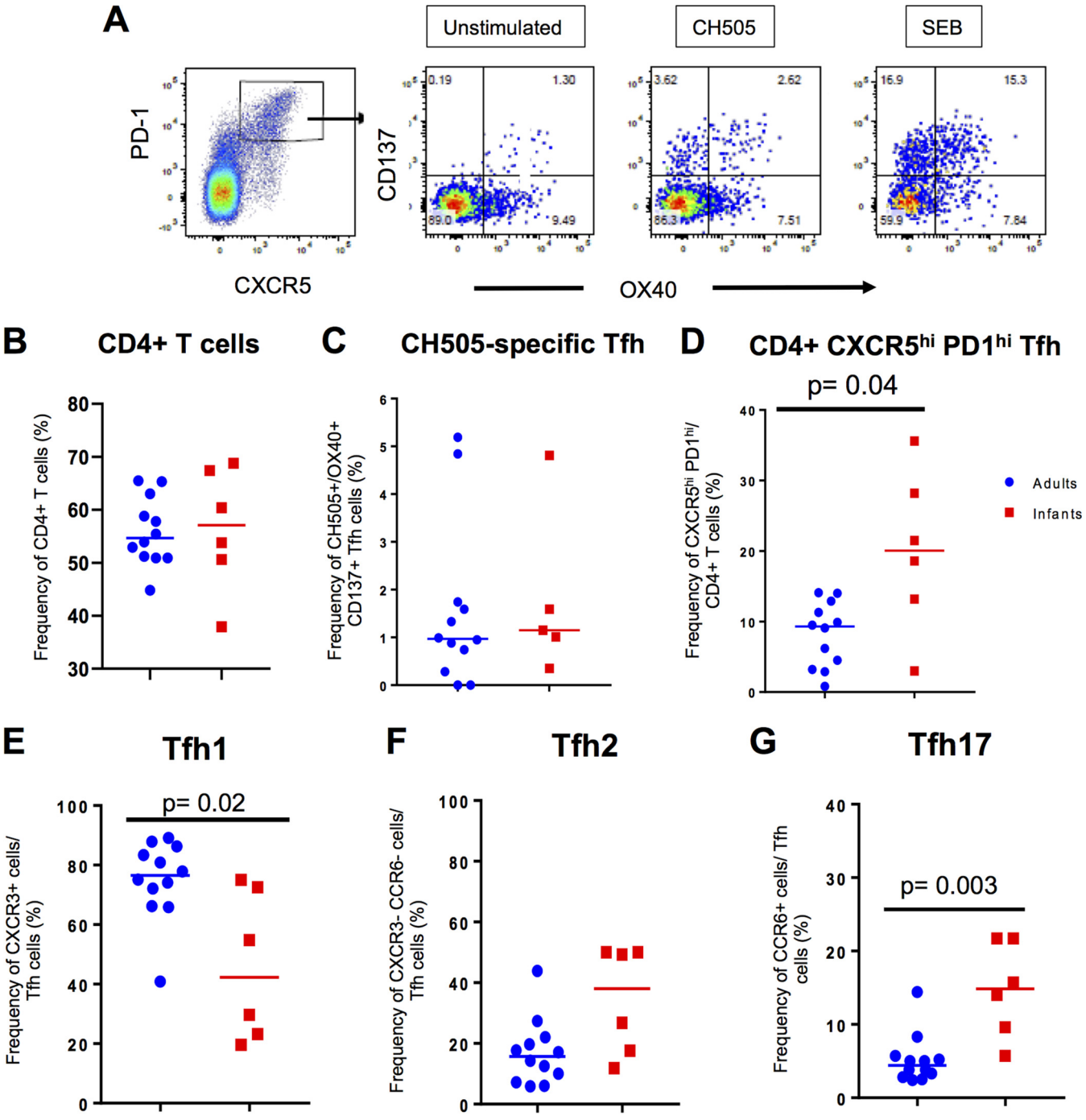

FIG 6 Frequencies of follicular T helper (Tfh) cells in the lymph node of SHIV.C.CH505-infected infant and adult monkeys at 12 wpi. Gating scheme for the AIM assay used to identify CH505-specific Tfh cells (A). Proportions of total $CD4^+$ T cells (A) and CH505-specific (B) and $CXCR5^{hi}$ $PD1^{hi}$ Tfh cells (C). Proportions of the Tfh subsets of $CXCR3^+$ Tfh1 (E), $CXCR3^-$ $CCR6^-$ Tfh2 (F), and $CCR6^+$ Tfh17 (G) cells. Each data point represents one animal, and medians are indicated as horizontal lines. FDR-adjusted *P* values are reported in the graphs, and an FDR *P* value of <0.05 was considered significant. See Tables S3 and S4 in the supplemental material for both unadjusted *P* and FDR *P* values for all comparisons.

ogous tier 2 neutralization-sensitive challenge virus CH505 T/F was not observed in the majority of monkeys from both age groups until 12 wpi (Fig. 8C). Eight out of 12 adults (66.7%) and 3 out of 6 infants (50%) developed autologous virus-neutralizing responses by 12 wpi, with no significant difference in potency (ID_{50} ranges of 45 to 161 for infants and 45 to 380 for adults [$P = 0.963$]) (Fig. 8C).

ADCC activity of plasma antibodies develops similarly in adult and infant acutely SHIV-infected monkeys. ADCC responses directed against CH505 gp120-

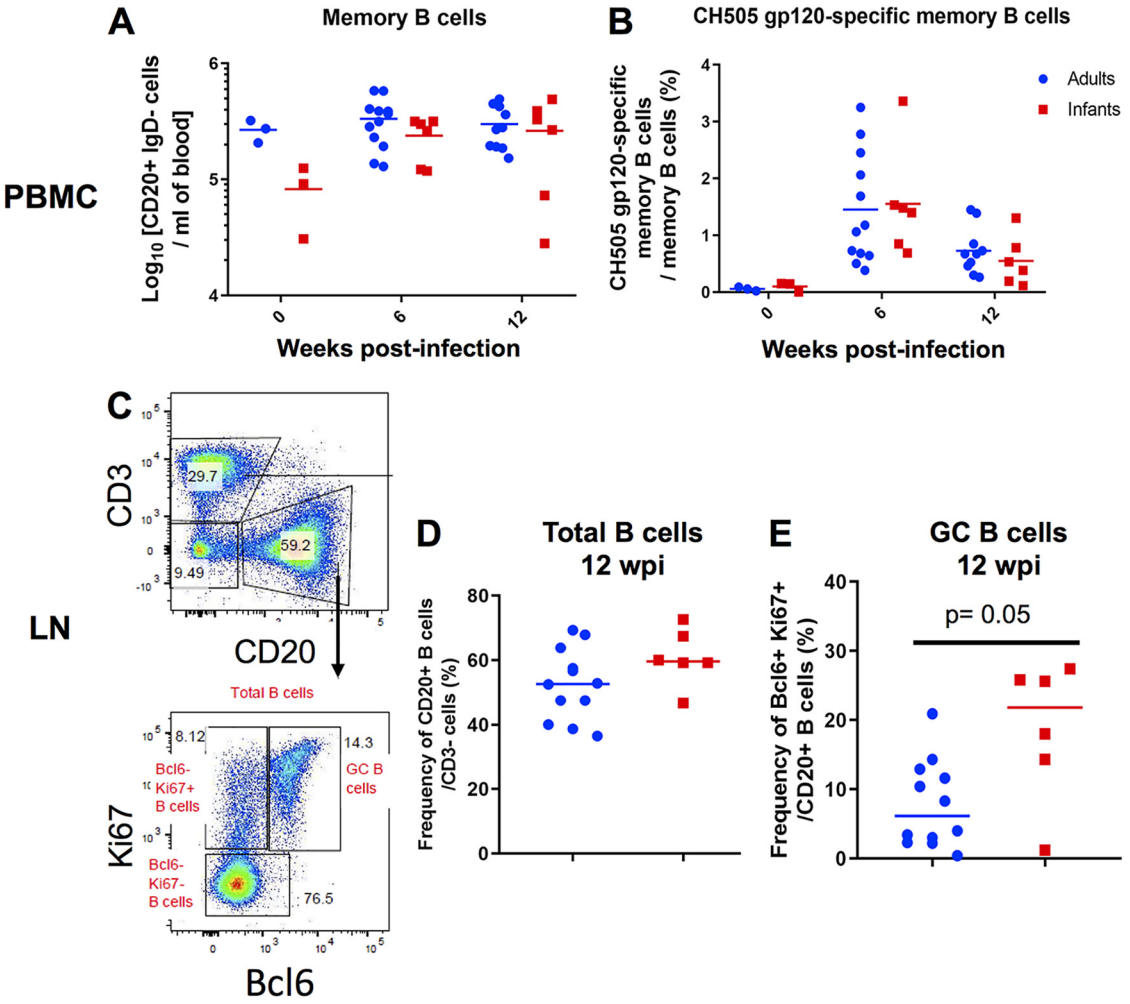

FIG 7 Similar proportions of systemic and lymph node B cell subsets in SHIV.C.CH505-infected infant and adult RMs. (A and B) Absolute counts of memory B cells (CD14$^-$ CD16$^-$ CD20$^+$ IgD$^-$ CD27 all) per milliliter of blood (A) and frequency of CH505 gp120-specific memory B cells of total memory B cells (B). (C to E) GC B cells were identified as CD20$^+$ Bcl6$^+$ Ki67$^+$ cells (C), and the frequencies of CD3$^-$ CD20$^+$ B cells (D) and CD20$^+$ Bcl6$^+$ Ki67$^+$ GC B cells (E) in the lymph node (LN) at 12 wpi are shown. Each data point represents one animal, and medians are indicated as horizontal lines. FDR-adjusted *P* values are reported in the graphs, and an FDR *P* value of <0.05 was considered significant. See Table S4 in the supplemental material for both unadjusted *P* and FDR *P* values for all comparisons.

coated target cells were measured using plasma samples collected from infant and adult RMs at 0, 6, and 10 wpi. ADCC activity was detectable in both age groups by week 6 of infection and was maintained through week 10, with no significant difference in the magnitude or kinetics of the response between the two groups (6 wpi, $P = 0.494$; 10 wpi, $P = 0.591$) (Fig. 9A). Additionally, similar kinetics were observed in the development of CH505-specific ADCC Ab titers in adults and infants, with no significant difference in magnitude (6 wpi, $P = 0.801$; 10 wpi, $P = 0.807$) (Fig. 9B).

Viral load at 12 wpi is significantly correlated with development of autologous virus neutralization in infant and adult monkeys. We calculated Spearman correlation coefficients to determine if a subset of the immunological responses assessed could predict the development of autologous neutralization in infant and adult monkeys at 12 wpi. CH505-specific gp120 IgG responses (rho = 0.69; $P = 0.002$; FDR $P = 0.07$) (Fig. 10B), ADCC antibody titers at 10 wpi (rho = 0.63; $P = 0.01$; FDR $P = 0.16$) (Fig. 9C), and CH505-specific Tfh cell frequencies at 12 wpi (rho = 0.49; $P = 0.05$; FDR $P = 0.19$) (Fig. 10D) were correlated with the development of autologous neutralization. However, these results were not statistically significant after adjustment for multiple comparisons. Yet the plasma viral load at 12 wpi was correlated with autologous

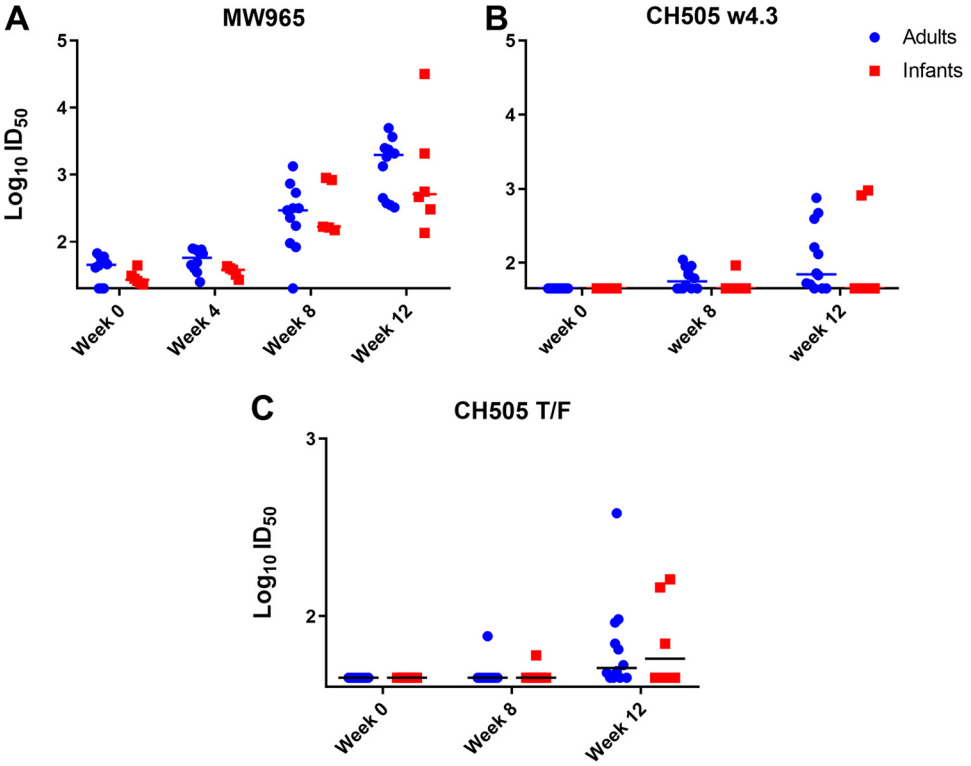

FIG 8 Magnitude and kinetics of plasma neutralization responses during acute SHIV.C.CH505 infection of infant and adult monkeys. A TZM-bl cell-based assay was performed to assess the neutralization activity of plasma antibodies. (A and B) Tier 1 neutralization responses were evaluated against MW965 (A) and CH505 w4.3 (B) through 12 wpi. (C) Autologous virus neutralization titers against CH505 T/F. Each dot represents plasma neutralization for one monkey, and medians are indicated as horizontal lines.

neutralization after adjustment for multiple comparisons (rho = 0.76; $P < 0.001$; FDR $P = 0.03$) (Fig. 10A). A summary of all the immune parameters assessed can be found in Fig. 11 and Table S1 in the supplemental material.

ADCC activity has been described to be important for a reduced risk of infection and/or viral control (7, 30, 34, 35) and has also been associated with levels of Env-specific IgG responses (34–37). Therefore, we calculated Spearman correlation coefficients to determine if a subset of the immunological parameters assessed was associated with the development of antibodies capable of mediating ADCC. Overall, none of the immune responses evaluated appeared to predict ADCC activity. A summary of all the immune parameters assessed can be found in Fig. 12 and Table S2.

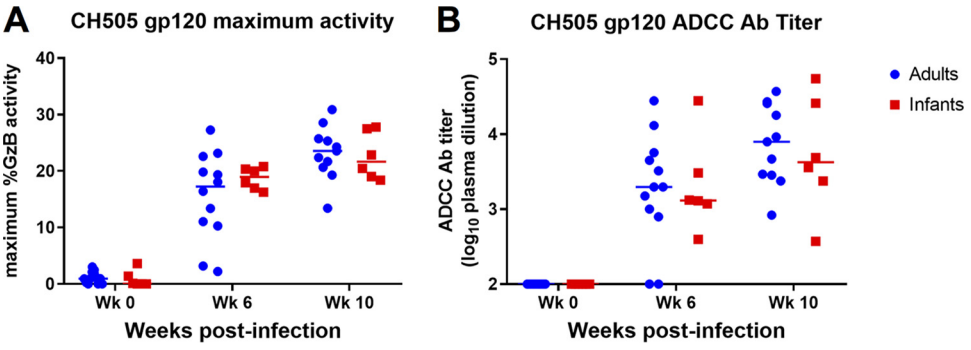

FIG 9 ADCC activity of plasma antibodies of SHIV.C.CH505-infected infant and adult monkeys. ADCC responses directed against CH505 gp120-coated target cells were measured at 0, 6, and 10 wpi. The maximum granzyme B activity (A) and plasma dilution endpoint antibody titers (B) for each animal are shown. Medians are indicated as horizontal lines.

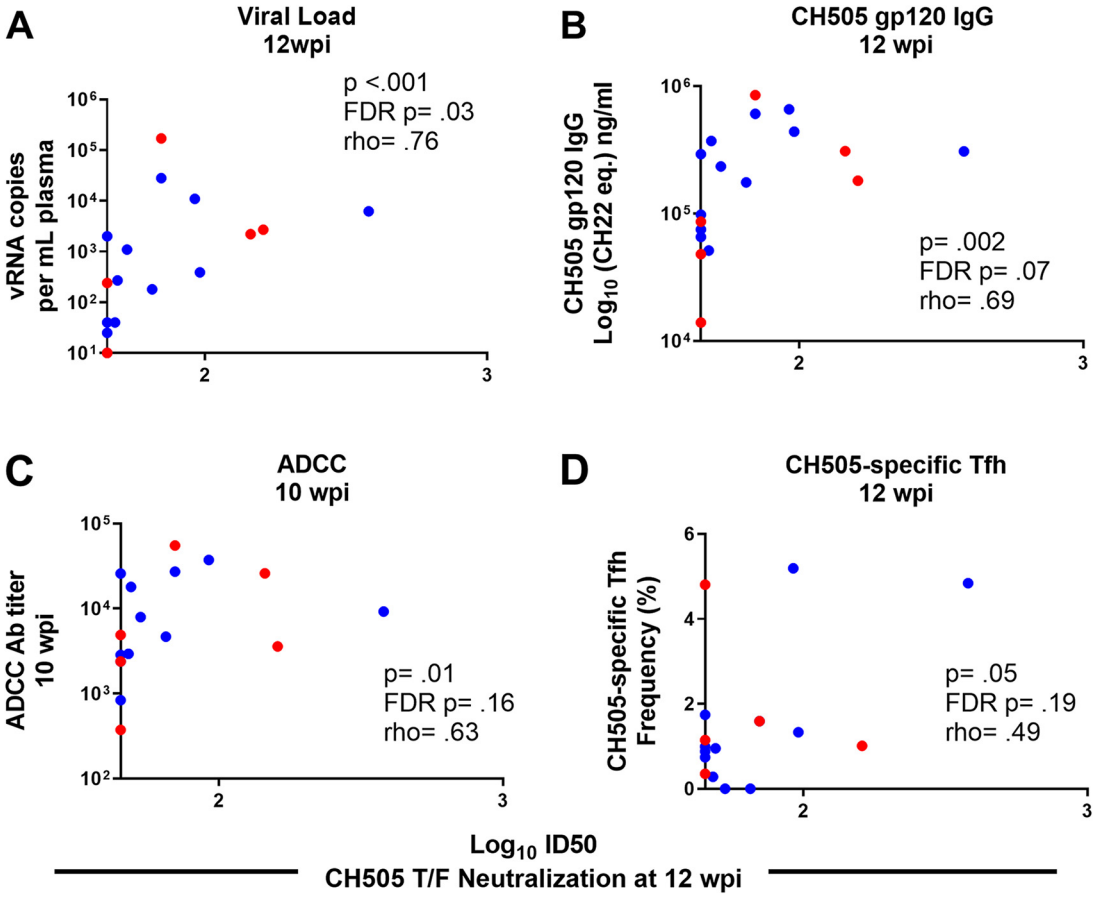

FIG 10 Viral load at 12 wpi is associated with development of autologous neutralization. Correlations between CH505 T/F neutralization at 12 wpi and plasma viral load at 12 wpi (A), CH505 gp120 IgG at 12 wpi (B), ADCC activity at 10 wpi (C), and frequency of CH505-specific Tfh cells at 12 wpi (D) are shown. The coefficients of correlation (rho [ρ]) and *P* values from testing whether the correlation coefficients differed significantly from zero are shown on the graphs. See Table S1 in the supplemental material for a complete list of immune parameters tested and correlation coefficients with both unadjusted *P* and FDR *P* values.

DISCUSSION

The elimination of pediatric HIV infections and achievement of lifelong immunity will likely require the development of successful immunization strategies tailored to the infant immune landscape. Thus, an understanding of the infant immune response and pathways for the development of neutralizing antibodies during HIV infection is critical to inform rational vaccine design. In this work, we utilized a clinically relevant rhesus macaque model of acute SHIV infection to better understand the development of HIV-specific immune responses in infants versus adults. The magnitude, kinetics, and specificity of HIV Env-specific plasma IgG responses were similar in SHIV.C.CH505 T/F-infected infant and adult monkeys. Furthermore, CH505 T/F-specific Tfh and memory B cell responses developed similarly in both age groups, consistent with the observed similarities in HIV Env-specific plasma IgG responses. However, infant monkeys exhibited significantly higher frequencies of total Tfh and GC B cells in lymph nodes during the early phase of infection. Moreover, acute SHIV.C.CH505 T/F infection elicited tier 2 autologous virus neutralization and ADCC responses that were similar in frequency and magnitude between both age groups. Finally, correlation analysis determined that the magnitude of the plasma viral load was the strongest predictor of the development of autologous virus neutralization in both age groups, consistent with previous reports in HIV-infected individuals (38).

A number of previous studies have demonstrated that differences exist between adult and pediatric immunity to HIV. A study of 46 HIV-infected human infants aged 0

A. Infants

Parameter	Correlation	P-Value
Viral load at 2wpi	-0.15	0.83
Viral load at 12wpi	0.77	0.11
MW965 neutralization at 12wpi	0.46	0.35
CH505 gp120 binding at 12wpi	0.7	0.17
ADCC titer at 10wpi	0.46	0.35
CD4 absolute counts at 10 wpi	-0.88	0.05
CD4+ central memory - prechallenge	0.39	0.45
CD4+ effector memory - prechallenge	-0.03	1
CD4+ naïve - prechallenge	0.58	0.25
CD4+ transitional memory- prechallenge	0.09	0.88
CD4+ CCR5+ - prechallenge	0.09	0.88
CD4+ CD69+ - prechallenge	-0.21	0.73
CD4+ HLADR+ - prechallenge	-0.46	0.35
CD4+ Ki67+ at 10 wpi	0.03	1
CH505-specific Tfh at 12wpi	0.31	0.6
CXCR5hi PD1hi Tfh at 12wpi	0.58	0.25
Tfh1 at 12wpi	0.7	0.17
Tfh17 at 12wpi	-0.7	0.17
Tfh2 at 12wpi	-0.7	0.17
Bcl6+ Ki67+ GC B cells at 12wpi	0.76	0.12

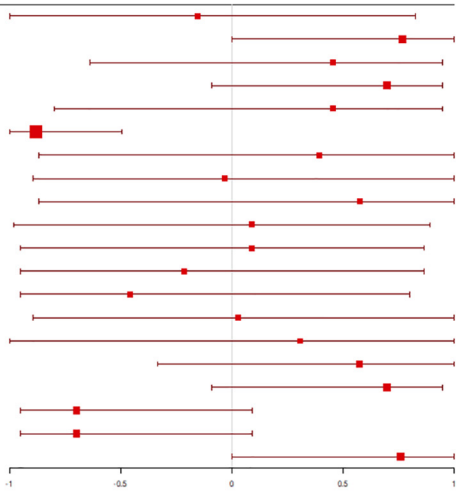

B. Adults

Parameter	Correlation	P-Value
Viral load at 2wpi	0.65	0.03
Viral load at 12wpi	0.69	0.02
MW965 neutralization at 12wpi	0.63	0.03
CH505 gp120 binding at 12wpi	0.7	0.01
ADCC titer at 10wpi	0.64	0.04
CD4 absolute counts at 10 wpi	0.49	0.11
CD4+ central memory - prechallenge	0.09	0.79
CD4+ effector memory - prechallenge	-0.19	0.55
CD4+ naïve - prechallenge	-0.12	0.71
CD4+ transitional memory- prechallenge	-0.04	0.91
CD4+ CCR5+ - prechallenge	0.28	0.37
CD4+ CD69+ - prechallenge	0.28	0.37
CD4+ HLADR+ - prechallenge	0.33	0.3
CD4+ Ki67+ at 10 wpi	0.58	0.05
CH505-specific Tfh at 12wpi	0.37	0.23
CXCR5hi PD1hi Tfh at 12wpi	0.56	0.06
Tfh1 at 12wpi	0.57	0.05
Tfh17 at 12wpi	-0.2	0.52
Tfh2 at 12wpi	-0.6	0.04
Bcl6+ Ki67+ GC B cells at 12wpi	0.59	0.05

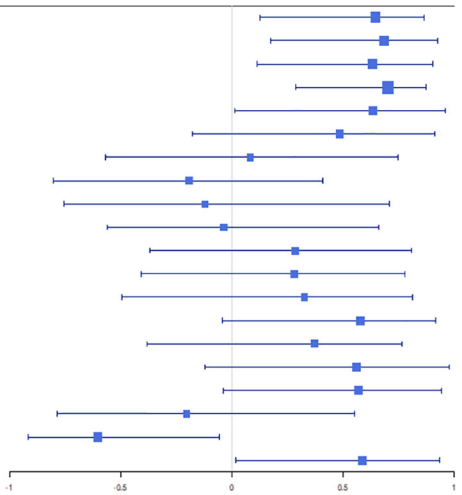

C. Overall

Parameter	Correlation	P-Value
Viral load at 2wpi	0.24	0.33
Viral load at 12wpi	0.76	0.0004*
MW965 neutralization at 12wpi	0.58	0.01
CH505 gp120 binding at 12wpi	0.69	0.0023
ADCC titer at 10wpi	0.63	0.01
CD4 absolute counts at 10 wpi	-0.05	0.85
CD4+ central memory - prechallenge	0.06	0.8
CD4+ effector memory - prechallenge	-0.15	0.56
CD4+ naïve - prechallenge	-0.14	0.59
CD4+ transitional memory- prechallenge	-0.03	0.91
CD4+ CCR5+ - prechallenge	0.12	0.65
CD4+ CD69+ - prechallenge	0	0.99
CD4+ HLADR+ - prechallenge	0.01	0.97
CD4+ Ki67+ at 10 wpi	0.29	0.24
CH505-specific Tfh at 12wpi	0.49	0.05
CXCR5hi PD1hi Tfh at 12wpi	0.49	0.04
Tfh1 at 12wpi	0.32	0.2
Tfh17 at 12wpi	-0.17	0.49
Tfh2 at 12wpi	-0.37	0.13
Bcl6+ Ki67+ GC B cells at 12wpi	0.54	0.02

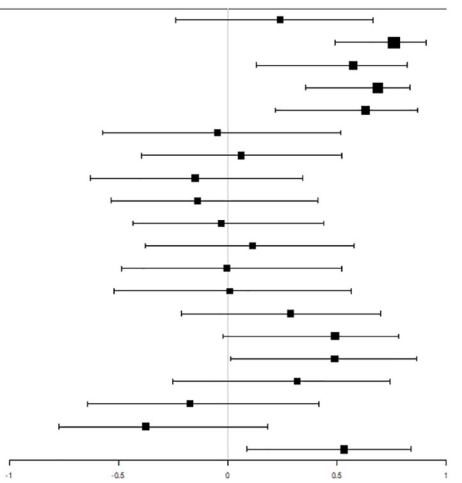

FIG 11 Summary correlation analysis of immune responses with autologous neutralization at 12 wpi. Forest plots of Spearman correlation coefficients of autologous virus neutralization at 12 wpi with various immune parameters in infant RMs (A), adult RMs (B), and both age groups (C) are shown.

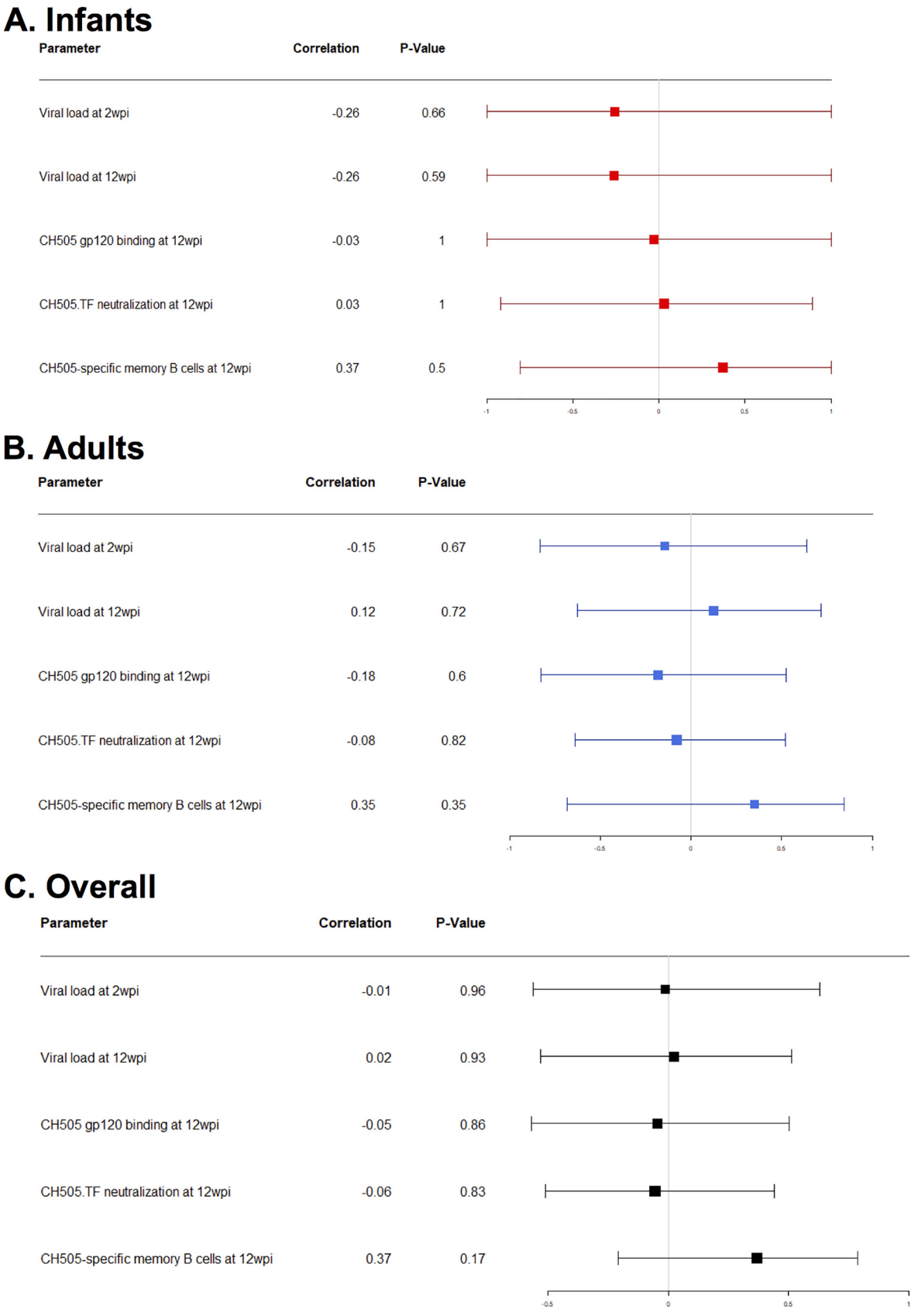

FIG 12 Summary correlation analysis of immune responses with ADCC at 10 wpi. Forest plots of Spearman correlations for ADCC at 10 wpi with various immune parameters in infant RMs (A), adult RMs (B), and both age groups (C) are shown.

to 12 months suggests that infants develop antibodies against gp160 first, followed by anti-gp120 and -gp41 antibodies (12). However, the initial Env-specific antibody responses in HIV-infected adults target gp41 and are nonneutralizing (11). While we observed similar kinetics of anti-gp120 plasma IgG antibodies in SHIV.C.CH505-infected infant and adult monkeys, gp41-specific responses exhibited a trend toward lower magnitude in the infant monkeys. Autologous virus neutralization responses also developed similarly in SHIV.C.CH505-infected adult and infant monkeys, with at least 50% of animals from both age groups exhibiting this response at 12 wpi (Fig. 8C). In human adults, autologous virus neutralization develops approximately 3 to 6 months after infection (39–43), while neutralization breadth develops after 2 to 3 years (19, 20). In infants, exactly when autologous virus-neutralizing antibodies develop is unknown, and such analysis is difficult due to the presence of maternal antibodies. However, it has recently been recognized that chronically HIV-infected infants can develop bnAbs as early as 1 to 2 years postinfection (14). If our results are reflective of what is happening in humans, they suggest that the initial kinetics of Env-specific antibody responses are comparable between adults and infants but that infants subsequently acquire neutralization breadth faster than adults and by distinct mechanisms. Interestingly, only plasma viral load was identified as a determinant of tier 2 autologous virus neutralization development among SHIV.C.CH505-infected infant and adult monkeys, suggesting that the development of autologous neutralization may be dependent upon antigen load. Further studies are needed to fully identify predictors of autologous neutralization, particularly since this response precedes the development of bnAbs in some individuals (22, 44, 45).

$CD4^+$ Tfh cells are crucial in providing help to B cells in the germinal center (GC) to support antibody maturation (46) and have been shown to be associated with the development of bnAbs during SHIV infection (47), in HIV-infected adults (17), and, more recently, in HIV-infected children (33). A recent study of HIV-1 clade C vertically infected human children and adults demonstrated that frequencies of total Tfh ($CXCR5^+$ $PD1^{hi}$) and HIV-specific (Gag/Env), IL-21-producing GC Tfh cells in oral lymphoid tissue were increased in older children receiving ART (age range, 6 to 10 years); however, it is unknown whether this is true in early life (33). Similarly, in our monkey model, we observed higher frequencies of total lymphoid Tfh and GC B cells in SHIV-infected infants than in adults at 12 wpi (Fig. 6D and Fig. 7E). Yet both age groups exhibited similar CH505-specific Tfh cell frequencies at 12 wpi (Fig. 6C), corresponding to similar magnitudes of CH505 gp120 IgG binding responses (Fig. 2A) and systemic memory B cell responses (Fig. 7A and B). The quality of these Tfh cell responses may not be optimal early in infection, as we observed that only about 50% of the monkeys in both age groups developed autologous virus neutralization responses by 12 wpi. Furthermore, the differences in Tfh and GC B cells may not be unique to SHIV infection, as the frequencies of lymphoid-resident Tfh cells are also higher in uninfected children than in uninfected adults (33).

Tfh cells can further be characterized into distinct functional subsets, namely, Tfh1 ($CXCR3^+$), Tfh2 ($CXCR3^-$ $CCR6^-$), and Tfh17 ($CCR6^+$) (48). Preferential enhancement of Tfh1 cells in the blood and lymph node have been observed in chronic SIV infection (49, 50), yet a recent study reported the expansion of Tfh2 subsets during acute HIV infection in adults (51). We observed that during acute SHIV infection, adult monkeys exhibited significantly higher frequencies of Tfh1 cells, whereas frequencies of Tfh17 cells were significantly higher in infants (Fig. 6E and G). Thus, acute SHIV infection induces a distinct Tfh phenotype in infants and adults. It is possible that distinctions in HIV immunity within our infant cohort are a result of maturation of the immune response rather than SHIV infection; thus, future studies would need to include an age-matched infant control group. Nonetheless, imbalances in Tfh cell polarization have been described in HIV-infected human children and adults. For example, a recent study showed that acute HIV infection in adults skews the distribution of circulating Tfh cell subsets toward the Tfh1 and Tfh2 phenotype compared to HIV-negative controls. Furthermore, frequencies of Tfh1 cells negatively correlated with set point viral loads

but positively correlated with plasma HIV-specific IgG responses in these adults (51). In addition, one study found that frequencies of PD1$^+$ CXCR3$^-$ CXCR5$^+$ Tfh subsets, which include both Tfh2 and Tfh17 cells, were predictive of the ability to develop bnAbs in acute HIV-1 infection of adults (52). More importantly, a Tfh2 bias was observed in HIV-infected children compared with adults (33). Finally, studies in both humans and nonhuman primates suggest that Th1-biased Tfh cell responses in chronic infection impair optimal B cell activity (49, 53, 54). These observations suggest that differential induction of Tfh subsets is important in developing potent HIV humoral immune responses. To improve our understanding of the role of Tfh phenotypes in the development of autologous virus neutralization and neutralization breadth, future studies would need to monitor SHIV-infected macaques for a longer time and longitudinally assess Tfh cell populations in parallel with assessing neutralization responses.

Clinically relevant SHIV infection models are essential in guiding our understanding of the induction of HIV Env-specific antibody responses. Furthermore, a preclinical model of infant HIV infection is critical to inform both early-life HIV vaccine strategies and pediatric HIV cure models. Our results demonstrate that SHIV.C.CH505.375H.dCT can infect infant macaques via repeated oral exposure; however, viral replication was not sustained through 12 wpi, and a true viral "set point" was not observed, in contrast to the slow decline in plasma viral loads observed in pediatric HIV infection (3). This lack of persistent viremia, which is characteristic of ART-naive, HIV-infected infants, represents one limitation of this SHIV model and warrants further optimization, potentially through additional viral modifications to escape natural control.

Our results suggest that the humoral immune response to SHIV infection develops similarly in adult and infant RMs and corroborate findings in human cohorts demonstrating that infants can develop robust HIV Env binding and neutralizing antibody responses despite their maturing immune landscape. Additionally, we have demonstrated that the Tfh landscape during acute infection in infants is distinct from that in adults, which may offer a potential advantage for infant vaccination, especially since studies suggest that infants are able to mount robust antibody responses to HIV Env vaccination, and these responses tend to be comparable or superior to those of adults (55–58). However, gaps in our knowledge still exist when it comes to understanding the infant immune response to HIV infection and how it can be harnessed for optimal vaccine-mediated protection against HIV-1. Thus, further development of infant SHIV models that depict human HIV-1 immunopathogenesis are imperative to enhance our understanding of infant HIV immunity and to inform vaccine elicitation of long-term protective immunity.

MATERIALS AND METHODS

Animal care and sample collection. Adult female rhesus macaques ranged from 4 to 10 years of age, and infant rhesus macaques ranged from 6 weeks of age (Table 1). All macaques were of Indian origin and from the type D retrovirus-free, SIV-free, and simian T cell leukemia virus type 1 (STLV-1)-free colony of the California National Primate Research Center (CNPRC) (Davis, CA). Animals were maintained in accordance with American Association for Accreditation of Laboratory Animal Care standards and the *Guide for the Care and Use of Laboratory Animals* (59). For sample collections, animals were sedated with ketamine HCl (Parke-Davis) injected at 10 mg/kg of body weight. EDTA-anticoagulated blood was collected via peripheral venipuncture. Plasma was separated from whole blood by centrifugation, and PBMCs were isolated by density gradient centrifugation using Ficoll-Paque (Sigma) or lymphocyte separation medium (MP Biomedicals). All protocols were reviewed and approved by the University of California, Davis, Institutional Animal Care and Use Committee (IACUC) prior to the initiation of the study.

SHIV challenge of infant and adult monkeys. The generation of SHIV.C.CH505.375H.dCT was previously described (20). The SHIV.C.CH505.375H.dCT challenge stock (provided by George M. Shaw, University of Pennsylvania) was prepared by infecting primary activated Indian rhesus macaque CD4$^+$ T cells, and 7 to 14 days later, culture supernatants were pooled, as previously described (20). Virus titers were determined in TZM-bl cells, yielding 6.8×10^6 $TCID_{50}$/ml.

Twelve adult monkeys were challenged intravenously with SHIV.C.CH505 at a dose of 3.4×10^5 $TCID_{50}$ (Table 1). Six infants were challenged orally beginning at 4 weeks of age. Initially, infants were exposed to SHIV.C.CH505 three times per day for 5 days at a dose of 8.5×10^4 $TCID_{50}$/ml in an isotonic sucrose solution and bottle-fed, in order to simulate oral acquisition via breastfeeding. After 1 week, only one infant became infected, and the remaining five infants were challenged 3 weeks later under sedation at a dose of 6.8×10^5 $TCID_{50}$/ml until infected. After 3 weeks, one infant remained uninfected and thus was subsequently challenged with an increasing dose (3.4×10^6 $TCID_{50}$/ml) until infected (Table 1).

Viral RNA load quantification. Plasma RNA load was quantified using a well-established quantitative reverse transcriptase PCR (RT-PCR) assay targeting SIVgag RNA, as previously described (20). RNA was isolated from plasma samples using the QIAsymphony Virus/Bacteria Midi kit on the QIAsymphony SP automated sample preparation platform (Qiagen, Hilden, Germany). RNA was extracted manually if plasma volumes were limited. Data reported are the numbers of SIV RNA copy equivalents per milliliter of plasma, with a limit of detection of 15 copies/ml.

Lymphocyte counts. Absolute lymphocyte counts in blood were calculated using the PBMC counts obtained by automated complete blood counts, multiplied by the lymphocyte percentages.

Enzyme-linked immunosorbent assay, recombinant protein, and soluble CD4 blocking. Env binding IgG was assessed in plasma in a 384-well-plate format. The plates were coated overnight with HIV CH505 gp120 (30 ng/well) or MN gp41 (3 μg/ml) and then blocked with the assay diluent (phosphate-buffered saline [PBS] containing 4% whey, 15% normal goat serum, and 0.5% Tween 20). Serially diluted plasma samples were then added to the plates and incubated for 1 h, followed by detection with a horseradish peroxidase (HRP)-conjugated antibody, polyclonal goat anti-monkey IgG (Rockland Immunochemicals). The plates were developed by using the 2,2′-azino-bis(3-ethylbenzothiazoline-6-sulphonic acid) (ABTS-2) peroxidase substrate system (KPL). The monoclonal antibody b12R1 was used to develop standard curves, and the concentration of IgG antibody was calculated relative to the standard using a 5-parameter fit curve (SoftMax Pro 7). For monoclonal antibodies, the 50% effective concentration (EC_{50}) was calculated as the concentration of antibody which resulted in a 50% reduction in the optical density (OD) from the maximum value.

For CD4-blocking enzyme-linked immunosorbent assays (ELISAs), 384-well plates (Corning Life Sciences) were coated with C.1086 gp120 at 30 ng/well. Following the same steps as the ones stated above, plates were blocked with assay diluent, and serially diluted monoclonal antibody and plasma were added and incubated for 1 h. Soluble CD4 (sCD4) (NIH AIDS Reagent Program, Division of AIDS, NIAID, NIH [human soluble CD4 recombinant protein from Progenics]) was then added at a concentration of 0.64 μg/ml. sCD4 binding was detected using biotinylated human anti-CD4 (Thermo Fisher Scientific) followed by HRP-conjugated streptavidin. Percent sCD4 binding inhibition was calculated as follows: 100 $-$ (average of serum duplicate OD/average of negative-control OD) $\times$ 100. A reduction of absorbance by $>$50% by Abs present in plasma indicated blocking of sCD4 binding to C.1086 gp120. The monoclonal antibody VRC01, which was used as a standard in this assay, has CD4 binding-site specificity and exhibits 80% blocking of sCD4 binding.

Binding antibody multiplex assay. HIV-1 epitope specificity and breadth were determined using a BAMA, as previously described (11). HIV-1 antigens were conjugated to polystyrene beads (Bio-Rad) as previously described (18), and binding of IgG to the bead-conjugated HIV-1 antigens was then measured in plasma samples from the infant and adult monkey cohorts. The positive control was purified IgG from pooled plasma of HIV Env-vaccinated rhesus macaques (RIVIG) (60). The conjugated beads were incubated on filter plates (Millipore) for approximately 30 min before plasma samples were added. The plasma samples were diluted in assay diluent (1% dry milk–5% goat serum–0.05% Tween 20 in 1$\times$ phosphate-buffered saline [pH 7.4]) at a 1:500 dilution. Beads and diluted samples were incubated for 30 min, and IgG binding was then detected using phycoerythrin (PE)-conjugated mouse anti-monkey IgG (Southern Biotech) at 4 μg/ml. The beads were washed and acquired on a Bio-Plex 200 instrument (Bio-Rad), and IgG binding was expressed as the mean fluorescence intensity (MFI). To assess the assay background, the MFI of binding to wells that did not contain beads or a sample (blank wells) and nonspecific binding of the samples to unconjugated blank beads were evaluated during assay analysis. High background detection for plasma samples was noted, and assays were repeated if necessary. An HIV envelope-specific antibody response was considered positive if it was above the lower limit of detection (MFI value of 100). To check for consistency between assays, the EC_{50} and maximum MFI values of the positive control (RIVIG) were tracked by Levy-Jennings charts. The antigens conjugated to the polystyrene beads are as follows: C.1086 gp140, C.1086 gp120, A1.Con_env03 gp140, A233 gp120, B.Con_env03 gp140, Con6 gp120, ConC gp120, MN gp120, linear V2.B, V3.C, C5.2.C, C1, conformational V1V2, ConC V3, MN V3, and C.1086 V1V2 (see Table S1 in the supplemental material).

Linear peptide microarray mapping and data analysis. Solid-phase peptide microarray epitope mapping was performed as previously described (61), with minor modifications. Briefly, JPT Peptide Technologies GmbH (Germany) prepares arrays slides by printing a library designed by B. Korber, Los Alamos National Laboratory, onto epoxy glass slides (PolyAn GmbH, Germany). The library contains 15-mer peptides overlapping by 12 residues, covering consensus Env (gp160) of clades A, B, C, and D; group M; CRF1; and CRF2 and vaccine strains (gp120) 1.A244, 1.TH023, MN, C.1086, C.TV1, and C.ZM651. To assess CH505-specific responses, a peptide library containing 59 CH505 strains (gp120, gp145, gp160, and SOSIP [sequences provided by Barton Haynes, Duke University]) was also designed (22). Sera were diluted 1:50 and applied to the peptide array, followed by washing and detection using goat anti-human IgG-Alexa Fluor 647 (AF647). Array slides were scanned at a wavelength of 635 nm with an InnoScan 710 AL scanner (Innopsys, France) using the XDR mode. Scan images were analyzed using MagPix 8.0 software to obtain binding intensity values for all peptides. Microarray data were then processing using the R package pepStat (62) to obtain a binding signal for each peptide, which is defined as $\log_2$(intensity of the sample at 12 wpi/intensity of the matched baseline sample). The magnitude of binding to each identified epitope is defined as the highest binding signal by a single peptide within the epitope region.

Neutralization assays. Neutralization by antibodies in plasma of MW965.LucR.T2A.ecto/293T IMC (clade C, tier 1), CH505 w4.3 HIV-1 pseudovirus (clade C, tier 1a), and autologous CH505 T/F (clade C, tier 2) HIV-1 pseudovirus was measured in TZM-bl cells (NIH AIDS Reagent Program, Division of AIDS, NIAID, NIH [from John Kappes]) via a reduction in luciferase reporter gene expression after a single round of

infection as previously described (63–65). Prior to screening, plasma was heat inactivated at 56°C for 30 min. Luminescence was measured using a Victor X3 multilabel plate reader, at 1 s per well (Perkin-Elmer). The ID_{50} was calculated as the dilution that resulted in a 50% reduction in relative luminescence units (RLU) compared to virus control wells. The monoclonal antibody b12R1 was used as a positive control for MW965 assays, and VRC01 was used a positive control for all other assays.

ADCC. The ADCC-GranToxiLux (GTL) assay was used to measure plasma ADCC activity as previously described (66). Briefly, CEM.NKR_{CCR5} target cells (NIH AIDS Reagent Program, Division of AIDS, NIAID, NIH [from Alexandra Trkola]) (67) were coated with recombinant CH505 gp120. Cryopreserved human PBMCs from an HIV-1-seronegative donor with the heterozygous 158 F/V genotype for Fcγ receptor IIIa were used as the source of effector cells (68, 69). Adult and infant plasma samples were tested after 4-fold serial dilution starting at 1:100. ADCC was measured as percent granzyme B (GzB) activity, defined as the frequency of target cells positive for proteolytically active GzB out of the total viable target cell population. Final results are expressed after subtraction of the background GzB activity observed in wells containing target and effector cells in the absence of plasma. ADCC endpoint titers were determined by interpolating the last positive dilution of plasma (>8% GzB activity).

Antigen-specific T cell responses. HIV gp120-specific T cell responses were measured as described previously (70). Briefly, thawed cells were enumerated, and 2×10^6 cells in suspension were cultivated in complete RPMI (RPM1 1640 with glutamine [Gibco] plus 10% heat-inactivated fetal bovine serum [FBS] [Serum Source International, Charlotte, NC] and 1× penicillin-streptomycin [Sigma-Aldrich, St. Louis, MO]) and stimulated with (i) no stimulant, (ii) 0.5× cell stimulation cocktail (eBioscience), or (iii) 10 μg of a consensus C HIV gp120 peptide pool (NIH AIDS Reagent Program) for 6 h, with 1× brefeldin A (eBioscience) present after the first hour. Cell preparations were then stained with a viability dye, and the following antibodies were used: CD3 allophycocyanin (APC)-Cy7 (clone SP34-2), CD4 PE-CF594 (L200), CD8 BV786 (RPA-T8), CD45RA V450 (5H9), CCR7 PE-Cy7 (3D12), IFN-γ AF700 (B27), IL-2 peridinin chlorophyll protein (PerCP)-Cy5.5 (MQ1-17H12), IL-17 PE (eBio64CAP17; eBioscience), and TNF-α APC (Mab11) (all antibodies were manufactured by BD Biosciences unless otherwise indicated). A minimum of 300,000 paraformaldehyde-fixed lymphocyte events were acquired on a BD LSR Fortessa instrument using FACSDiva v8.0 software. Data were analyzed using FlowJo software v10.5.3 (TreeStar, Ashland, OR).

CH505 envelope-specific memory B cell phenotyping. For phenotyping of CH505 Env-specific memory B cells, a suspension of 10^6 PBMCs was blocked with 6.25 μg/ml anti-human CD4 antibody (BD Biosciences) at 4°C for 15 min. After incubation, PBMCs were washed twice with PBS and pelleted at 1,500 rpm for 5 min. PBMCs were then incubated at 4°C with a Live/Dead fixable aqua dead cell stain kit (Thermo Fisher Scientific) for 30 min. Following incubation and washing with PBS, PBMCs were then stained with a cocktail of fluorescently conjugated antibodies for surface markers, including CD20 fluorescein isothiocyanate (FITC) (clone L27), CD3 PerCP-Cy5.5 (SP34-2), IgM PE-Cy5 (G20-127), CD16 PE-Cy7 (3G8), CD8 PE-Texas Red (3B5), IgD PE (polyclonal), CD14 BV570 (M5E2), CD27 APC-Cy7 (O323), and custom-conjugated BV421–HIV-1 gp120 (C.CH505 T/F) and AF647–HIV-1 gp120 (C.CH505 T/F), prepared as described previously (71). The stained PBMCs were acquired on an LSRII flow cytometer (BD Biosciences) using BD FACSDiva software and analyzed as described above. The following gating strategy was applied: lymphocytes were gated on singlets, and live cells were selected to gate on $CD3^-$ cells (T cells), $CD14^-$ cells (monocytes/macrophages), and $CD20^+$ cells (B cells). B cells were further gated on $CD27^+$ memory B cells. Only B cells positive for both BV421-gp120 and AF647-gp120 were considered CH505-Env specific.

Lymph node Tfh phenotyping and activation-induced marker assay. The activation-induced marker (AIM) assay was based on previous work (72). Briefly, cryopreserved rhesus macaque lymph node cells (12 wpi) were thawed, rested for 3 h at 37°C with 5% CO_2, resuspended in AIM V medium (Gibco), and transferred at 10^6 cells per well to a 24-well plate. Cells were cultured for 18 h at 37°C with 5% CO_2, with no exogenous stimulation (negative control) or with gp140 stimulation (5 μg/ml CH505 T/F gp140 protein and 0.5 μg/ml of a 15-mer peptide pool with an 11-residue overlap spanning CH505 T/F gp140). As a positive control, cells were stimulated with 0.5 μg/ml staphylococcal enterotoxin B (SEB) (Sigma). Duplicates for each condition were performed when cell numbers permitted. Following stimulation, cells were labeled with fluorescently labeled antibodies to the following surface antigens: PD1 BV421 (clone EH12.2H7), CD8a BV570 (RPA-T8), CD25 BV650 (BC96), CD4 BV711 (OKT4), CD69 PE-Cy5 (FN50), CD45RA FITC (MEM-56), CD137 AF647 (4B4-1), and CD185 PE-Cy7 (MU5UBEE) (BioLegend) as well as CD3 APC-Cy7 (clone SP34-2), CD20 FITC (L27), CD196 PerCP-Cy5.5 (11A9), OX40 PE (L106), and CD183 PE-CF594 (1C6/CXCR3) (BD Biosciences). For Tfh phenotyping, the following gating strategy was applied (Fig. 6A): lymphocytes were gated on singlets, and live cells were selected to gate on $CD4^+$ $CXCR5^+$ $Foxp3^-$ cells, followed by gating on CCR6 and CXCR3. Cell viability was measured using Live/Dead fixable aqua stain (eBioscience). Flow cytometry data were acquired on an LSRII instrument running FACSDiva software (BD Biosciences) and analyzed as described above.

Statistical methods. Immune assay measurements at various time points postinfection and the change in immune assay measurements from the baseline were compared between SHIV-infected infant and adult monkeys using Wilcoxon rank sum tests with exact *P* values. Spearman's rank correlation coefficients were estimated for the cohort as a whole as well as by adult monkeys and infants separately. All correlations were tested with exact *P* values to assess whether any were significantly different from zero. To adjust for multiple comparisons, the Benjamini-Hochberg (BH) procedure was used to control the false discovery rate (FDR). Separate adjustments to control the FDR at an α value of 0.05 were performed for comparisons between the infant and adult monkeys using (i) the prespecified primary endpoints for a total of 26 tests (Table S3), (ii) the prespecified secondary endpoints for a total of 43 tests (Table S4), (iii) correlations between prespecified parameters and CH505 T/F neutralization at 12 wpi for

a total of 60 tests (Table S1), and (iv) correlations between prespecified parameters and ADCC minus percent GzB activity at 10 weeks postinfection for a total of 15 tests (Table S2). Both the unadjusted *P* values (raw *P*) and FDR-adjusted *P* values (FDR *P*) are reported in the supplemental material. All statistical tests were performed using SAS version 9.4 (SAS Institute, Cary, NC, USA).

SUPPLEMENTAL MATERIAL

Supplemental material for this article may be found at https://doi.org/10.1128/JVI.00168-19.

SUPPLEMENTAL FILE 1, XLS file, 0.03 MB.
SUPPLEMENTAL FILE 2, XLS file, 0.03 MB.
SUPPLEMENTAL FILE 3, XLS file, 0.03 MB.
SUPPLEMENTAL FILE 4, XLS file, 0.03 MB.

ACKNOWLEDGMENTS

The work was supported by National Institutes of Health grants P01 AI117915 (S.R.P. and K.D.P.), T32 CA009111 (A.N.N.), 5R01 AI106380 (S.R.P.), 5R01-DE025444 (S.R.P.), and T32 5108303 (A.D.C.). This work was also supported by the Penn Center for AIDS Research Viral and Molecular Core (P30 AI045008 [K.B.]) the BEAT-HIV: Delaney Collaboratory To Cure HIV-1 Infection by Combination Immunotherapy (UM1AI126620 [K.B.]), and CARE: Delaney Collaboratory for AIDS Eradication (UM1AI126619 [K.B.]). Research reported in this publication was supported by the University of North Carolina Center for AIDS Research under award number 5P30AI050410 (K.D.P.). Flow cytometry was performed in the Duke Human Vaccine Institute Flow Cytometry Facility (Durham, NC) and the UNC Flow Cytometry Core Facility, which is supported in part by Cancer Center core support grant P30 CA016086 (UNC Lineberger Comprehensive Cancer Center). We are also thankful for statistical support for this study provided by the Center for AIDS Research at the University of North Carolina at Chapel Hill, an NIH-funded program (P30 AI50410).

We thank George Shaw, University of Pennsylvania Department of Medicine, Philadelphia, PA, for providing us with SHIV.C.CH505.375H.dCT. Protein antigens for BAMAs and ELISAs were generously provided by Kevin Saunders and Barton Haynes, supported by NIH NIAID Division of AIDS UM1 grant AI100645 for the Center for HIV/AIDS Vaccine Immunology-Immunogen Discovery (CHAVI-ID) and produced at the DHVI Protein Production Facility. Study data were collected and managed using REDCap (Research Electronic Data Capture) electronic data capture tools hosted at Duke University. We thank Jeff Lifson, Rebecca Shoemaker, and colleagues in the Quantitative Molecular Diagnostics Core of the AIDS and Cancer Virus Program of the Frederick National Laboratory for expert assistance with viral load measurements. We also thank J. Watanabe, J. Usachenko, A. Ardeshir, and the staff of the CNPRC Colony Research Services for their support in these studies. We thank Georgia Tomaras' laboratory for technical support with the linear epitope mapping microarray. We thank R. Whitney Edwards and Nicole Rodgers for technical assistance with ADCC assays.

The funders had no role in study design, data collection and interpretation, or the decision to submit the work for publication. The content is solely the responsibility of the authors and does not necessarily represent the official views of the National Institutes of Health.

REFERENCES

1. UNAIDS. 2017. UNAIDS global fact sheet. UNAIDS, Geneva, Switzerland.
2. UNAIDS. 2016. Global plan towards the elimination of new HIV infections among children by 2015 and keeping their mothers alive. UNAIDS, Geneva, Switzerland.
3. Martinez DR, Permar SR, Fouda GG. 2016. Contrasting adult and infant immune responses to HIV infection and vaccination. Clin Vaccine Immunol 23:84–94. https://doi.org/10.1128/CVI.00565-15.
4. Goulder PJ, Lewin SR, Leitman EM. 2016. Paediatric HIV infection: the potential for cure. Nat Rev Immunol 16:259–271. https://doi.org/10.1038/nri.2016.19.
5. Richardson BA, Mbori-Ngacha D, Lavreys L, John-Stewart GC, Nduati R, Panteleeff DD, Emery S, Kreiss JK, Overbaugh J. 2003. Comparison of human immunodeficiency virus type 1 viral loads in Kenyan women, men, and infants during primary and early infection. J Virol 77:7120–7123. https://doi.org/10.1128/jvi.77.12.7120-7123.2003.
6. Muenchhoff M, Prendergast AJ, Goulder PJ. 2014. Immunity to HIV in early life. Front Immunol 5:391. https://doi.org/10.3389/fimmu.2014.00391.
7. Becquet R, Marston M, Dabis F, Moulton LH, Gray G, Coovadia HM, Essex M, Ekouevi DK, Jackson D, Coutsoudis A, Kilewo C, Leroy V, Wiktor SZ, Nduati R, Msellati P, Zaba B, Ghys PD, Newell ML, UNAIDS Child Survival Group. 2012. Children who acquire HIV infection perinatally are at higher risk of early death than those acquiring infection through breastmilk: a meta-analysis. PLoS One 7:e28510. https://doi.org/10.1371/journal.pone.0028510.

8. Marinda E, Humphrey JH, Iliff PJ, Mutasa K, Nathoo KJ, Piwoz EG, Moulton LH, Salama P, Ward BJ, ZVITAMBO Study Group. 2007. Child mortality according to maternal and infant HIV status in Zimbabwe. Pediatr Infect Dis J 26:519–526. https://doi.org/10.1097/01.inf.0000264527.69954.4c.
9. Marston M, Becquet R, Zaba B, Moulton LH, Gray G, Coovadia H, Essex M, Ekouevi DK, Jackson D, Coutsoudis A, Kilewo C, Leroy V, Wiktor S, Nduati R, Msellati P, Dabis F, Newell ML, Ghys PD. 2011. Net survival of perinatally and postnatally HIV-infected children: a pooled analysis of individual data from sub-Saharan Africa. Int J Epidemiol 40:385–396. https://doi.org/10.1093/ije/dyq255.
10. Ferrand RA, Corbett EL, Wood R, Hargrove J, Ndhlovu CE, Cowan FM, Gouws E, Williams BG. 2009. AIDS among older children and adolescents in Southern Africa: projecting the time course and magnitude of the epidemic. AIDS 23:2039–2046. https://doi.org/10.1097/QAD.0b013e32833016ce.
11. Tomaras GD, Yates NL, Liu P, Qin L, Fouda GG, Chavez LL, Decamp AC, Parks RJ, Ashley VC, Lucas JT, Cohen M, Eron J, Hicks CB, Liao HX, Self SG, Landucci G, Forthal DN, Weinhold KJ, Keele BF, Hahn BH, Greenberg ML, Morris L, Karim SS, Blattner WA, Montefiori DC, Shaw GM, Perelson AS, Haynes BF. 2008. Initial B-cell responses to transmitted human immunodeficiency virus type 1: virion-binding immunoglobulin M (IgM) and IgG antibodies followed by plasma anti-gp41 antibodies with ineffective control of initial viremia. J Virol 82:12449–12463. https://doi.org/10.1128/JVI.01708-08.
12. Pollack H, Zhan MX, Ilmet-Moore T, Ajuang-Simbiri K, Krasinski K, Borkowsky W. 1993. Ontogeny of anti-human immunodeficiency virus (HIV) antibody production in HIV-1-infected infants. Proc Natl Acad Sci U S A 90:2340–2344. https://doi.org/10.1073/pnas.90.6.2340.
13. Henrard D, Fauvel M, Samson J, Delage G, Boucher M, Hankins C, Stephens J, Lapointe N. 1993. Ontogeny of the humoral immune response to human immunodeficiency virus type 1 in infants. J Infect Dis 168:288–291. https://doi.org/10.1093/infdis/168.2.288.
14. Goo L, Chohan V, Nduati R, Overbaugh J. 2014. Early development of broadly neutralizing antibodies in HIV-1-infected infants. Nat Med 20:655–658. https://doi.org/10.1038/nm.3565.
15. deCamp A, Hraber P, Bailer RT, Seaman MS, Ochsenbauer C, Kappes J, Gottardo R, Edlefsen P, Self S, Tang H, Greene K, Gao H, Daniell X, Sarzotti-Kelsoe M, Gorny MK, Zolla-Pazner S, LaBranche CC, Mascola JR, Korber BT, Montefiori DC. 2014. Global panel of HIV-1 Env reference strains for standardized assessments of vaccine-elicited neutralizing antibodies. J Virol 88:2489–2507. https://doi.org/10.1128/JVI.02853-13.
16. Simonich CA, Williams KL, Verkerke HP, Williams JA, Nduati R, Lee KK, Overbaugh J. 2016. HIV-1 neutralizing antibodies with limited hypermutation from an infant. Cell 166:77–87. https://doi.org/10.1016/j.cell.2016.05.055.
17. Muenchhoff M, Adland E, Karimanzira O, Crowther C, Pace M, Csala A, Leitman E, Moonsamy A, McGregor C, Hurst J, Groll A, Mori M, Sinmyee S, Thobakgale C, Tudor-Williams G, Prendergast AJ, Kloverpris H, Roider J, Leslie A, Shingadia D, Brits T, Daniels S, Frater J, Willberg CB, Walker BD, Ndung'u T, Jooste P, Moore PL, Morris L, Goulder P. 2016. Nonprogressing HIV-infected children share fundamental immunological features of nonpathogenic SIV infection. Sci Transl Med 8:358ra125. https://doi.org/10.1126/scitranslmed.aag1048.
18. Milligan C, Richardson BA, John-Stewart G, Nduati R, Overbaugh J. 2015. Passively acquired antibody-dependent cellular cytotoxicity (ADCC) activity in HIV-infected infants is associated with reduced mortality. Cell Host Microbe 17:500–506. https://doi.org/10.1016/j.chom.2015.03.002.
19. Broliden K, Sievers E, Tovo PA, Moschese V, Scarlatti G, Broliden PA, Fundaro C, Rossi P. 1993. Antibody-dependent cellular cytotoxicity and neutralizing activity in sera of HIV-1-infected mothers and their children. Clin Exp Immunol 93:56–64. https://doi.org/10.1111/j.1365-2249.1993.tb06497.x.
20. Li H, Wang S, Kong R, Ding W, Lee FH, Parker Z, Kim E, Learn GH, Hahn P, Policicchio B, Brocca-Cofano E, Deleage C, Hao X, Chuang GY, Gorman J, Gardner M, Lewis MG, Hatziioannou T, Santra S, Apetrei C, Pandrea I, Alam SM, Liao HX, Shen X, Tomaras GD, Farzan M, Chertova E, Keele BF, Estes JD, Lifson JD, Doms RW, Montefiori DC, Haynes BF, Sodroski JG, Kwong PD, Hahn BH, Shaw GM. 2016. Envelope residue 375 substitutions in simian-human immunodeficiency viruses enhance CD4 binding and replication in rhesus macaques. Proc Natl Acad Sci U S A 113:E3413–E3422. https://doi.org/10.1073/pnas.1606636113.
21. Gao F, Bonsignori M, Liao HX, Kumar A, Xia SM, Lu X, Cai F, Hwang KK, Song H, Zhou T, Lynch RM, Alam SM, Moody MA, Ferrari G, Berrong M, Kelsoe G, Shaw GM, Hahn BH, Montefiori DC, Kamanga G, Cohen MS, Hraber P, Kwong PD, Korber BT, Mascola JR, Kepler TB, Haynes BF. 2014. Cooperation of B cell lineages in induction of HIV-1-broadly neutralizing antibodies. Cell 158:481–491. https://doi.org/10.1016/j.cell.2014.06.022.
22. Liao H-X, Lynch R, Zhou T, Gao F, Alam SM, Boyd SD, Fire AZ, Roskin KM, Schramm CA, Zhang Z, Zhu J, Shapiro L, NISC Comparative Sequencing Program, Mullikin JC, Gnanakaran S, Hraber P, Wiehe K, Kelsoe G, Yang G, Xia S-M, Montefiori DC, Parks R, Lloyd KE, Scearce RM, Soderberg KA, Cohen M, Kamanga G, Louder MK, Tran LM, Chen Y, Cai F, Chen S, Moquin S, Du X, Joyce MG, Srivatsan S, Zhang B, Zheng A, Shaw GM, Hahn BH, Kepler TB, Korber BTM, Kwong PD, Mascola JR, Haynes BF. 2013. Co-evolution of a broadly neutralizing HIV-1 antibody and founder virus. Nature 496:469–476. https://doi.org/10.1038/nature12053.
23. Nelson AN, Goswami R, Dennis M, Tu J, Mangan RJ, Saha PT, Cain DW, Curtis AD, Shen X, Shaw GM, Bar K, Hudgens M, Pollara J, De Paris K, Van Rompay KKA, Permar SR. 2019. SHIV.CH505-infected infant and adult rhesus macaques exhibit similar HIV Env-specific antibody kinetics, despite distinct T-follicular helper (Tfh) and germinal center B cell landscapes. bioRxiv https://doi.org/10.1101/538876.
24. Abel K, Pahar B, Van Rompay KK, Fritts L, Sin C, Schmidt K, Colon R, McChesney M, Marthas ML. 2006. Rapid virus dissemination in infant macaques after oral simian immunodeficiency virus exposure in the presence of local innate immune responses. J Virol 80:6357–6367. https://doi.org/10.1128/JVI.02240-05.
25. Marthas ML, Van Rompay KK, Abbott Z, Earl P, Buonocore-Buzzelli L, Moss B, Rose NF, Rose JK, Kozlowski PA, Abel K. 2011. Partial efficacy of a VSV-SIV/MVA-SIV vaccine regimen against oral SIV challenge in infant macaques. Vaccine 29:3124–3137. https://doi.org/10.1016/j.vaccine.2011.02.051.
26. Hartigan-O'Connor DJ, Abel K, McCune JM. 2007. Suppression of SIV-specific CD4+ T cells by infant but not adult macaque regulatory T cells: implications for SIV disease progression. J Exp Med 204:2679–2692. https://doi.org/10.1084/jem.20071068.
27. McMichael AJ, Borrow P, Tomaras GD, Goonetilleke N, Haynes BF. 2010. The immune response during acute HIV-1 infection: clues for vaccine development. Nat Rev Immunol 10:11–23. https://doi.org/10.1038/nri2674.
28. DeMaria MA, Casto M, O'Connell M, Johnson RP, Rosenzweig M. 2000. Characterization of lymphocyte subsets in rhesus macaques during the first year of life. Eur J Haematol 65:245–257. https://doi.org/10.1034/j.1600-0609.2000.065004245.x.
29. Marthas ML, van Rompay KK, Otsyula M, Miller CJ, Canfield DR, Pedersen NC, McChesney MB. 1995. Viral factors determine progression to AIDS in simian immunodeficiency virus-infected newborn rhesus macaques. J Virol 69:4198–4205.
30. Van Rompay KK, Greenier JL, Cole KS, Earl P, Moss B, Steckbeck JD, Pahar B, Rourke T, Montelaro RC, Canfield DR, Tarara RP, Miller C, McChesney MB, Marthas ML. 2003. Immunization of newborn rhesus macaques with simian immunodeficiency virus (SIV) vaccines prolongs survival after oral challenge with virulent SIVmac251. J Virol 77:179–190. https://doi.org/10.1128/jvi.77.1.179-190.2003.
31. Bohm RP, Jr, Martin LN, Davison-Fairburn B, Baskin GB, Murphey-Corb M. 1993. Neonatal disease induced by SIV infection of the rhesus monkey (Macaca mulatta). AIDS Res Hum Retroviruses 9:1131–1137. https://doi.org/10.1089/aid.1993.9.1131.
32. Thobakgale CF, Ramduth D, Reddy S, Mkhwanazi N, de Pierres C, Moodley E, Mphatswe W, Blanckenberg N, Cengimbo A, Prendergast A, Tudor-Williams G, Dong K, Jeena P, Kindra G, Bobat R, Coovadia H, Kiepiela P, Walker BD, Goulder PJ. 2007. Human immunodeficiency virus-specific CD8+ T-cell activity is detectable from birth in the majority of in utero-infected infants. J Virol 81:12775–12784. https://doi.org/10.1128/JVI.00624-07.
33. Roider J, Maehara T, Ngoepe A, Ramsuran D, Muenchhoff M, Adland E, Aicher T, Kazer SW, Jooste P, Karim F, Kuhn W, Shalek AK, Ndung'u T, Morris L, Moore PL, Pillai S, Kloverpris H, Goulder P, Leslie A. 2018. High-frequency, functional HIV-specific T-follicular helper and regulatory cells are present within germinal centers in children but not adults. Front Immunol 9:1975. https://doi.org/10.3389/fimmu.2018.01975.
34. Baum LL, Cassutt KJ, Knigge K, Khattri R, Margolick J, Rinaldo C, Kleeberger CA, Nishanian P, Henrard DR, Phair J. 1996. HIV-1 gp120-specific antibody-dependent cell-mediated cytotoxicity correlates with rate of disease progression. J Immunol 157:2168–2173.
35. Forthal DN, Landucci G, Haubrich R, Keenan B, Kuppermann BD, Tilles JG, Kaplan J. 1999. Antibody-dependent cellular cytotoxicity independently predicts survival in severely immunocompromised human immunode-

ficiency virus-infected patients. J Infect Dis 180:1338–1341. https://doi.org/10.1086/314988.
36. Fouda GG, Yates NL, Pollara J, Shen X, Overman GR, Mahlokozera T, Wilks AB, Kang HH, Salazar-Gonzalez JF, Salazar MG, Kalilani L, Meshnick SR, Hahn BH, Shaw GM, Lovingood RV, Denny TN, Haynes B, Letvin NL, Ferrari G, Montefiori DC, Tomaras GD, Permar SR, Center for HIV/AIDS Vaccine Immunology. 2011. HIV-specific functional antibody responses in breast milk mirror those in plasma and are primarily mediated by IgG antibodies. J Virol 85:9555–9567. https://doi.org/10.1128/JVI.05174-11.
37. Gomez-Roman VR, Patterson LJ, Venzon D, Liewehr D, Aldrich K, Florese R, Robert-Guroff M. 2005. Vaccine-elicited antibodies mediate antibody-dependent cellular cytotoxicity correlated with significantly reduced acute viremia in rhesus macaques challenged with SIVmac251. J Immunol 174:2185–2189. https://doi.org/10.4049/jimmunol.174.4.2185.
38. Deeks SG, Schweighardt B, Wrin T, Galovich J, Hoh R, Sinclair E, Hunt P, McCune JM, Martin JN, Petropoulos CJ, Hecht FM. 2006. Neutralizing antibody responses against autologous and heterologous viruses in acute versus chronic human immunodeficiency virus (HIV) infection: evidence for a constraint on the ability of HIV to completely evade neutralizing antibody responses. J Virol 80:6155–6164. https://doi.org/10.1128/JVI.00093-06.
39. Arendrup M, Nielsen C, Hansen JE, Pedersen C, Mathiesen L, Nielsen JO. 1992. Autologous HIV-1 neutralizing antibodies: emergence of neutralization-resistant escape virus and subsequent development of escape virus neutralizing antibodies. J Acquir Immune Defic Syndr 5:303–307.
40. Aasa-Chapman MM, Hayman A, Newton P, Cornforth D, Williams I, Borrow P, Balfe P, McKnight A. 2004. Development of the antibody response in acute HIV-1 infection. AIDS 18:371–381. https://doi.org/10.1097/00002030-200402200-00002.
41. Li B, Decker JM, Johnson RW, Bibollet-Ruche F, Wei X, Mulenga J, Allen S, Hunter E, Hahn BH, Shaw GM, Blackwell JL, Derdeyn CA. 2006. Evidence for potent autologous neutralizing antibody titers and compact envelopes in early infection with subtype C human immunodeficiency virus type 1. J Virol 80:5211–5218. https://doi.org/10.1128/JVI.00201-06.
42. Tang H, Robinson JE, Gnanakaran S, Li M, Rosenberg ES, Perez LG, Haynes BF, Liao HX, Labranche CC, Korber BT, Montefiori DC. 2011. Epitopes immediately below the base of the V3 loop of gp120 as targets for the initial autologous neutralizing antibody response in two HIV-1 subtype B-infected individuals. J Virol 85:9286–9299. https://doi.org/10.1128/JVI.02286-10.
43. Wei X, Decker JM, Wang S, Hui H, Kappes JC, Wu X, Salazar-Gonzalez JF, Salazar MG, Kilby JM, Saag MS, Komarova NL, Nowak MA, Hahn BH, Kwong PD, Shaw GM. 2003. Antibody neutralization and escape by HIV-1. Nature 422:307–312. https://doi.org/10.1038/nature01470.
44. Frost SD, Wrin T, Smith DM, Kosakovsky Pond SL, Liu Y, Paxinos E, Chappey C, Galovich J, Beauchaine J, Petropoulos CJ, Little SJ, Richman DD. 2005. Neutralizing antibody responses drive the evolution of human immunodeficiency virus type 1 envelope during recent HIV infection. Proc Natl Acad Sci U S A 102:18514–18519. https://doi.org/10.1073/pnas.0504658102.
45. Bonsignori M, Pollara J, Moody MA, Alpert MD, Chen X, Hwang KK, Gilbert PB, Huang Y, Gurley TC, Kozink DM, Marshall DJ, Whitesides JF, Tsao CY, Kaewkungwal J, Nitayaphan S, Pitisuttithum P, Rerks-Ngarm S, Kim JH, Michael NL, Tomaras GD, Montefiori DC, Lewis GK, DeVico A, Evans DT, Ferrari G, Liao HX, Haynes BF. 2012. Antibody-dependent cellular cytotoxicity-mediating antibodies from an HIV-1 vaccine efficacy trial target multiple epitopes and preferentially use the VH1 gene family. J Virol 86:11521–11532. https://doi.org/10.1128/JVI.01023-12.
46. Crotty S. 2011. Follicular helper CD4 T cells (TFH). Annu Rev Immunol 29:621–663. https://doi.org/10.1146/annurev-immunol-031210-101400.
47. Yamamoto T, Lynch RM, Gautam R, Matus-Nicodemos R, Schmidt SD, Boswell KL, Darko S, Wong P, Sheng Z, Petrovas C, McDermott AB, Seder RA, Keele BF, Shapiro L, Douek DC, Nishimura Y, Mascola JR, Martin MA, Koup RA. 2015. Quality and quantity of TFH cells are critical for broad antibody development in SHIVAD8 infection. Sci Transl Med 7:298ra120. https://doi.org/10.1126/scitranslmed.aab3964.
48. Schmitt N, Bentebibel SE, Ueno H. 2014. Phenotype and functions of memory Tfh cells in human blood. Trends Immunol 35:436–442. https://doi.org/10.1016/j.it.2014.06.002.
49. Velu V, Mylvaganam G, Ibegbu C, Amara RR. 2018. Tfh1 cells in germinal centers during chronic HIV/SIV infection. Front Immunol 9:1272. https://doi.org/10.3389/fimmu.2018.01272.
50. Velu V, Mylvaganam GH, Gangadhara S, Hong JJ, Iyer SS, Gumber S, Ibegbu CC, Villinger F, Amara RR. 2016. Induction of Th1-biased T follicular helper (Tfh) cells in lymphoid tissues during chronic simian immunodeficiency virus infection defines functionally distinct germinal center Tfh cells. J Immunol 197:1832–1842. https://doi.org/10.4049/jimmunol.1600143.
51. Baiyegunhi O, Ndlovu B, Ogunshola F, Ismail N, Walker BD, Ndung'u T, Ndhlovu ZM. 2018. Frequencies of circulating Th1-biased T follicular helper cells in acute HIV-1 infection correlate with the development of HIV-specific antibody responses and lower set point viral load. J Virol 92:e00659-18. https://doi.org/10.1128/JVI.00659-18.
52. Locci M, Havenar-Daughton C, Landais E, Wu J, Kroenke MA, Arlehamn CL, Su LF, Cubas R, Davis MM, Sette A, Haddad EK, International AIDS Vaccine Initiative Protocol C Principal Investigators, Poignard P, Crotty S. 2013. Human circulating PD-1+CXCR3−CXCR5+ memory Tfh cells are highly functional and correlate with broadly neutralizing HIV antibody responses. Immunity 39:758–769. https://doi.org/10.1016/j.immuni.2013.08.031.
53. Cubas RA, Mudd JC, Savoye AL, Perreau M, van Grevenynghe J, Metcalf T, Connick E, Meditz A, Freeman GJ, Abesada-Terk G, Jr, Jacobson JM, Brooks AD, Crotty S, Estes JD, Pantaleo G, Lederman MM, Haddad EK. 2013. Inadequate T follicular cell help impairs B cell immunity during HIV infection. Nat Med 19:494–499. https://doi.org/10.1038/nm.3109.
54. Cubas R, van Grevenynghe J, Wills S, Kardava L, Santich BH, Buckner CM, Muir R, Tardif V, Nichols C, Procopio F, He Z, Metcalf T, Ghneim K, Locci M, Ancuta P, Routy JP, Trautmann L, Li Y, McDermott AB, Koup RA, Petrovas C, Migueles SA, Connors M, Tomaras GD, Moir S, Crotty S, Haddad EK. 2015. Reversible reprogramming of circulating memory T follicular helper cell function during chronic HIV infection. J Immunol 195:5625–5636. https://doi.org/10.4049/jimmunol.1501524.
55. Fouda GG, Cunningham CK, McFarland EJ, Borkowsky W, Muresan P, Pollara J, Song LY, Liebl BE, Whitaker K, Shen X, Vandergrift NA, Overman RG, Yates NL, Moody MA, Fry C, Kim JH, Michael NL, Robb M, Pitisuttithum P, Kaewkungwal J, Nitayaphan S, Rerks-Ngarm S, Liao HX, Haynes BF, Montefiori DC, Ferrari G, Tomaras GD, Permar SR. 2015. Infant HIV type 1 gp120 vaccination elicits robust and durable anti-V1V2 immunoglobulin G responses and only rare envelope-specific immunoglobulin A responses. J Infect Dis 211:508–517. https://doi.org/10.1093/infdis/jiu444.
56. Haynes BF, Gilbert PB, McElrath MJ, Zolla-Pazner S, Tomaras GD, Alam SM, Evans DT, Montefiori DC, Karnasuta C, Sutthent R, Liao HX, DeVico AL, Lewis GK, Williams C, Pinter A, Fong Y, Janes H, DeCamp A, Huang Y, Rao M, Billings E, Karasavvas N, Robb ML, Ngauy V, de Souza MS, Paris R, Ferrari G, Bailer RT, Soderberg KA, Andrews C, Berman PW, Frahm N, De Rosa SC, Alpert MD, Yates NL, Shen X, Koup RA, Pitisuttithum P, Kaewkungwal J, Nitayaphan S, Rerks-Ngarm S, Michael NL, Kim JH. 2012. Immune-correlates analysis of an HIV-1 vaccine efficacy trial. N Engl J Med 366:1275–1286. https://doi.org/10.1056/NEJMoa1113425.
57. Rerks-Ngarm S, Pitisuttithum P, Nitayaphan S, Kaewkungwal J, Chiu J, Paris R, Premsri N, Namwat C, de Souza M, Adams E, Benenson M, Gurunathan S, Tartaglia J, McNeil JG, Francis DP, Stablein D, Birx DL, Chunsuttiwat S, Khamboonruang C, Thongcharoen P, Robb ML, Michael NL, Kunasol P, Kim JH, MOPH-TAVEG Investigators. 2009. Vaccination with ALVAC and AIDSVAX to prevent HIV-1 infection in Thailand. N Engl J Med 361:2209–2220. https://doi.org/10.1056/NEJMoa0908492.
58. McGuire EP, Fong Y, Toote C, Cunningham CK, McFarland EJ, Borkowsky W, Barnett S, Itell HL, Kumar A, Gray G, McElrath MJ, Tomaras GD, Permar SR, Fouda GG. 2018. HIV-exposed infants vaccinated with an MF59/recombinant gp120 vaccine have higher-magnitude anti-V1V2 IgG responses than adults immunized with the same vaccine. J Virol 92:e01070-17. https://doi.org/10.1128/JVI.01070-17.
59. National Research Council. 2011. Guide for the care and use of laboratory animals, 8th ed. National Academies Press, Washington, DC. https://doi.org/10.17226/12910.
60. Phillips B, Fouda GG, Eudailey J, Pollara J, Curtis AD, II, Kunz E, Dennis M, Shen X, Bay C, Hudgens M, Pickup D, Alam SM, Ardeshir A, Kozlowski PA, Van Rompay KKA, Ferrari G, Moody MA, Permar S, De Paris K. 2017. Impact of poxvirus vector priming, protein coadministration, and vaccine intervals on HIV gp120 vaccine-elicited antibody magnitude and function in infant macaques. Clin Vaccine Immunol 24:e00231-17. https://doi.org/10.1128/CVI.00231-17.
61. Shen X, Duffy R, Howington R, Cope A, Sadagopal S, Park H, Pal R, Kwa S, Ding S, Yang OO, Fouda GG, Le Grand R, Bolton D, Esteban M, Phogat S, Roederer M, Amara RR, Picker LJ, Seder RA, McElrath MJ, Barnett S,

Permar SR, Shattock R, DeVico AL, Felber BK, Pavlakis GN, Pantaleo G, Korber BT, Montefiori DC, Tomaras GD. 2015. Vaccine-induced linear epitope-specific antibodies to simian immunodeficiency virus SIVmac239 envelope are distinct from those induced to the human immunodeficiency virus type 1 envelope in nonhuman primates. J Virol 89:8643–8650. https://doi.org/10.1128/JVI.03635-14.

62. Gottardo R, Bailer RT, Korber BT, Gnanakaran S, Phillips J, Shen X, Tomaras GD, Turk E, Imholte G, Eckler L, Wenschuh H, Zerweck J, Greene K, Gao H, Berman PW, Francis D, Sinangil F, Lee C, Nitayaphan S, Rerks-Ngarm S, Kaewkungwal J, Pitisuttithum P, Tartaglia J, Robb ML, Michael NL, Kim JH, Zolla-Pazner S, Haynes BF, Mascola JR, Self S, Gilbert P, Montefiori DC. 2013. Plasma IgG to linear epitopes in the V2 and V3 regions of HIV-1 gp120 correlate with a reduced risk of infection in the RV144 vaccine efficacy trial. PLoS One 8:e75665. https://doi.org/10.1371/journal.pone.0075665.
63. Sarzotti-Kelsoe M, Bailer RT, Turk E, Lin CL, Bilska M, Greene KM, Gao H, Todd CA, Ozaki DA, Seaman MS, Mascola JR, Montefiori DC. 2014. Optimization and validation of the TZM-bl assay for standardized assessments of neutralizing antibodies against HIV-1. J Immunol Methods 409:131–146. https://doi.org/10.1016/j.jim.2013.11.022.
64. Li M, Gao F, Mascola JR, Stamatatos L, Polonis VR, Koutsoukos M, Voss G, Goepfert P, Gilbert P, Greene KM, Bilska M, Kothe DL, Salazar-Gonzalez JF, Wei X, Decker JM, Hahn BH, Montefiori DC. 2005. Human immunodeficiency virus type 1 env clones from acute and early subtype B infections for standardized assessments of vaccine-elicited neutralizing antibodies. J Virol 79:10108–10125. https://doi.org/10.1128/JVI.79.16.10108-10125.2005.
65. Montefiori DC. 2009. Measuring HIV neutralization in a luciferase reporter gene assay. Methods Mol Biol 485:395–405. https://doi.org/10.1007/978-1-59745-170-3_26.
66. Pollara J, Hart L, Brewer F, Pickeral J, Packard BZ, Hoxie JA, Komoriya A, Ochsenbauer C, Kappes JC, Roederer M, Huang Y, Weinhold KJ, Tomaras GD, Haynes BF, Montefiori DC, Ferrari G. 2011. High-throughput quantitative analysis of HIV-1 and SIV-specific ADCC-mediating antibody responses. Cytometry A 79:603–612. https://doi.org/10.1002/cyto.a.21084.
67. Trkola A, Matthews J, Gordon C, Ketas T, Moore JP. 1999. A cell line-based neutralization assay for primary human immunodeficiency virus type 1 isolates that use either the CCR5 or the CXCR4 coreceptor. J Virol 73:8966–8974.
68. Bruhns P, Iannascoli B, England P, Mancardi DA, Fernandez N, Jorieux S, Daeron M. 2009. Specificity and affinity of human Fcgamma receptors and their polymorphic variants for human IgG subclasses. Blood 113:3716–3725. https://doi.org/10.1182/blood-2008-09-179754.
69. Koene HR, Kleijer M, Algra J, Roos D, von dem Borne AE, de Haas M. 1997. Fc gammaRIIIa-158V/F polymorphism influences the binding of IgG by natural killer cell Fc gammaRIIIa, independently of the Fc gammaRIIIa-48L/R/H phenotype. Blood 90:1109–1114.
70. Curtis AD, Il, Walter KA, Nabi R, Jensen K, Dwivedi A, Pollara J, Ferrari G, Van Rompay KKA, Amara RR, Kozlowski PA, De Paris K. 2019. Oral coadministration of an intramuscular DNA/modified vaccinia Ankara vaccine for simian immunodeficiency virus is associated with better control of infection in orally exposed infant macaques. AIDS Res Hum Retroviruses 35:310–325. https://doi.org/10.1089/aid.2018.0180.
71. Williams WB, Zhang J, Jiang C, Nicely NI, Fera D, Luo K, Moody MA, Liao HX, Alam SM, Kepler TB, Ramesh A, Wiehe K, Holland JA, Bradley T, Vandergrift N, Saunders KO, Parks R, Foulger A, Xia SM, Bonsignori M, Montefiori DC, Louder M, Eaton A, Santra S, Scearce R, Sutherland L, Newman A, Bouton-Verville H, Bowman C, Bomze H, Gao F, Marshall DJ, Whitesides JF, Nie X, Kelsoe G, Reed SG, Fox CB, Clary K, Koutsoukos M, Franco D, Mascola JR, Harrison SC, Haynes BF, Verkoczy L. 2017. Initiation of HIV neutralizing B cell lineages with sequential envelope immunizations. Nat Commun 8:1732. https://doi.org/10.1038/s41467-017-01336-3.
72. Reiss S, Baxter AE, Cirelli KM, Dan JM, Morou A, Daigneault A, Brassard N, Silvestri G, Routy JP, Havenar-Daughton C, Crotty S, Kaufmann DE. 2017. Comparative analysis of activation induced marker (AIM) assays for sensitive identification of antigen-specific CD4 T cells. PLoS One 12:e0186998. https://doi.org/10.1371/journal.pone.0186998.